NPS - 59CG73061A

NAVAL POSTGRADUATE SCHOOL

Monterey, California

AN ANALYTICAL MODEL FOR PREDICTING
THE DAILY TEMPERATURE CYCLE OF CONTAINER
STORED ORDNANCE

by

THOMAS E. COOPER
and
ALLEN H. WIRZBURGER

18 June 1973

Approved for public release; distribution unlimited.

NAVAL POSTGRADUATE SCHOOL
Monterey, California

Rear Admiral M. B. Freeman, USN
Superintendent

M. U. Clauser
Provost

ABSTRACT

The heat transfer characteristics of a container stored rocket motor have been investigated using analytical and experimental techniques. Comparison between analytically predicted and experimentally determined values of temperature are within the estimated experimental uncertainty of ±3°F. The results of the analytical solution may be used to predict maximum and minimum temperatures, thermal time lags, and temperature gradients throughout the rocket motor. For convenience, maximum temperature and time lag information is presented in nomograph form as a function of three parameters: normalized radial location, normalized frequency, and normalized gap conductance. These three parameters control the temperature behavior of the motor. It is proposed that the nomographs will be a useful tool for thermally optimizing future container designs.

This task was supported by: Naval Weapons Center, China Lake, California, Work Request No. 3-3006

TABLE OF CONTENTS

LIST OF TABLES

LIST OF ILLUSTRATIONS

Figure

I. INTRODUCTION

An analytical model is presented for predicting the daily temperature history of a container stored rocket motor. The model, which is developed using the method of complex temperatures [1, 2]*, assumes that heat is transferred only in the radial direction and that the container surface temperature is known a priori and varies sinusoidally with time. Comparison of theory with experiment is within experimental uncertainty (± 3°F) when temperature is interpreted as bulk temperature. The analytical model is especially useful for studying geometrical and thermophysical property effects on rocket motor temperature. Such parameter studies have been carried out and the results are presented in nomograph form.

II. BACKGROUND

In 1959 the Naval Weapons Center located at China Lake, California, recognized the need for a concerted attack on the problem of thermal criteria assignment for new weapon systems. In 1963 a task force was established to study the complete environmental criteria determination problem. The key to this problem seemed to be the thermal area in the storage and transportation events of any item. It was realized that transportation was a short term situation compared to the storage situation. Therefore, the major portion of the life of an item must be in storage. There are three types of storage; covered, igloo, and dump. The dump storage situation leads to the more extreme thermal exposure situations.

---

* Numbers in brackets designate references at end of report.

As data were not available for the dump storage situation, instrumented storage dumps were created at representative places on a worldwide basis so that statistical data could be obtained on a variety of ordnance. The first site was at China Lake, California, in the middle of the Mojave Desert. This site now has the capability of returning about 250 channels of information on a continuous temperature-time basis (Figure 1). Other arctic and tropical sites were set up to study extreme conditions.

In the experimental dump storage situation the ordnance is exposed singly, directly situated on the ground, with the long axis aligned in the north-south direction to allow maximum normal exposure of the container surface to the sun's rays. In actual practice, ordnance is usually stacked and oriented in other than a north-south direction, thereby avoiding the extreme temperature condition. Ordnance sitting on the ground receives terrestial radiation, cannot quickly give off heat by conduction to the soil, and is not as apt to be cooled by the prevailing breeze; therefore, extreme temperatures result.

The most important source of heat to the ordnance is the direct radiation from the sun, with terrestial radiation being of secondary importance. For extreme conditions to occur, the wind must be calm (less than 5 knots), the sky clear, and the outside air temperature high. After sunrise the ordnance skin temperature rises much more rapidly than the ambient air temperature; therefore, the surrounding air cools the ordnance, rather than heats it.

The rocket motors used for the tests were military surplus. Even though the material had served its intended in-Fleet purpose, it was still representative of new hardware, when viewed in a thermodynamic

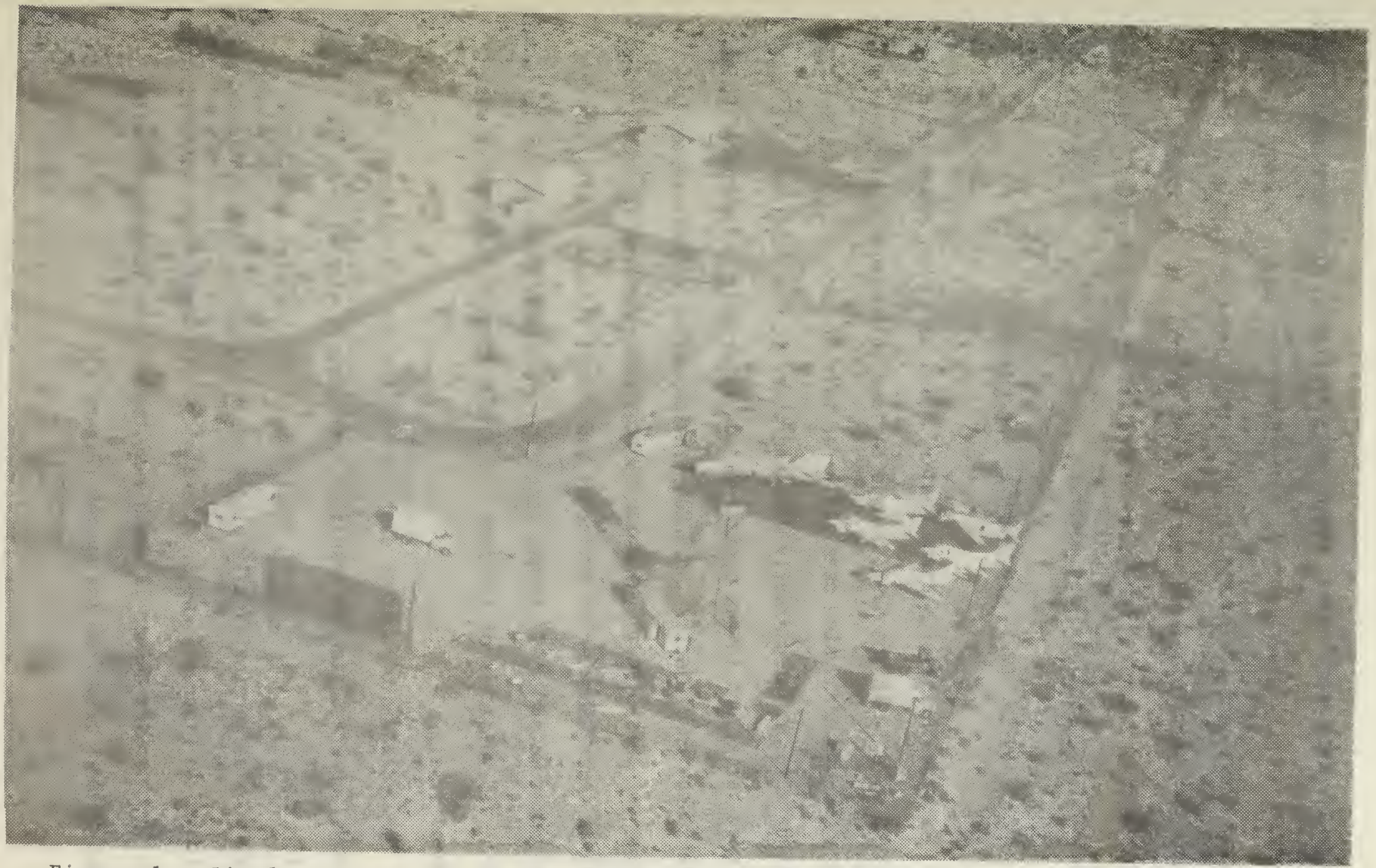

Figure 1. Simulated Storage Site at China Lake.

context. When inert rocket motors were available, they were used intact; however, in most cases, once-fired hardware was used. Thoroughly dried desert blown sand, being similar in thermal properties to most propellants, was used to backfill empty rocket motors. It was assumed that the thermal response of the sand filled motors was essentially the same as actual propellant filled motors.

III. EXPERIMENTAL PROCEDURE

Although the Naval Weapons Center, China Lake, had accumulated vast amounts of data in the past, it was decided to instrument a rocket motor storage container system especially for this project. This would allow base data to be taken exactly when and where it was required. It also allowed variations in the system without interfering with one of China Lake's ongoing projects. An ASROC (antisubmarine rocket) system was chosen for this study. The outer storage container was 75 inches long with an inner diameter of 18 inches and a wall thickness of 1/16 inch. The rocket motor was 57 inches long with an outside diameter of 12 inches and a wall thickness of 1/4 inch. Both the container and motor were made of steel.

The rocket motor storage container system was instrumented with 20 gage copper-constantan insulated thermocouple wire with an ISA calibration of ± 1-1/2°F over the range -75 to +200°F. Twenty-one thermocouples were originally placed on the system. Positions are indicated in Figures 2 and 3. The ambient air temperature was measured with thermocouple number 19 which was located in a Stevenson shelter about 60 feet away from the system (Figure 4).

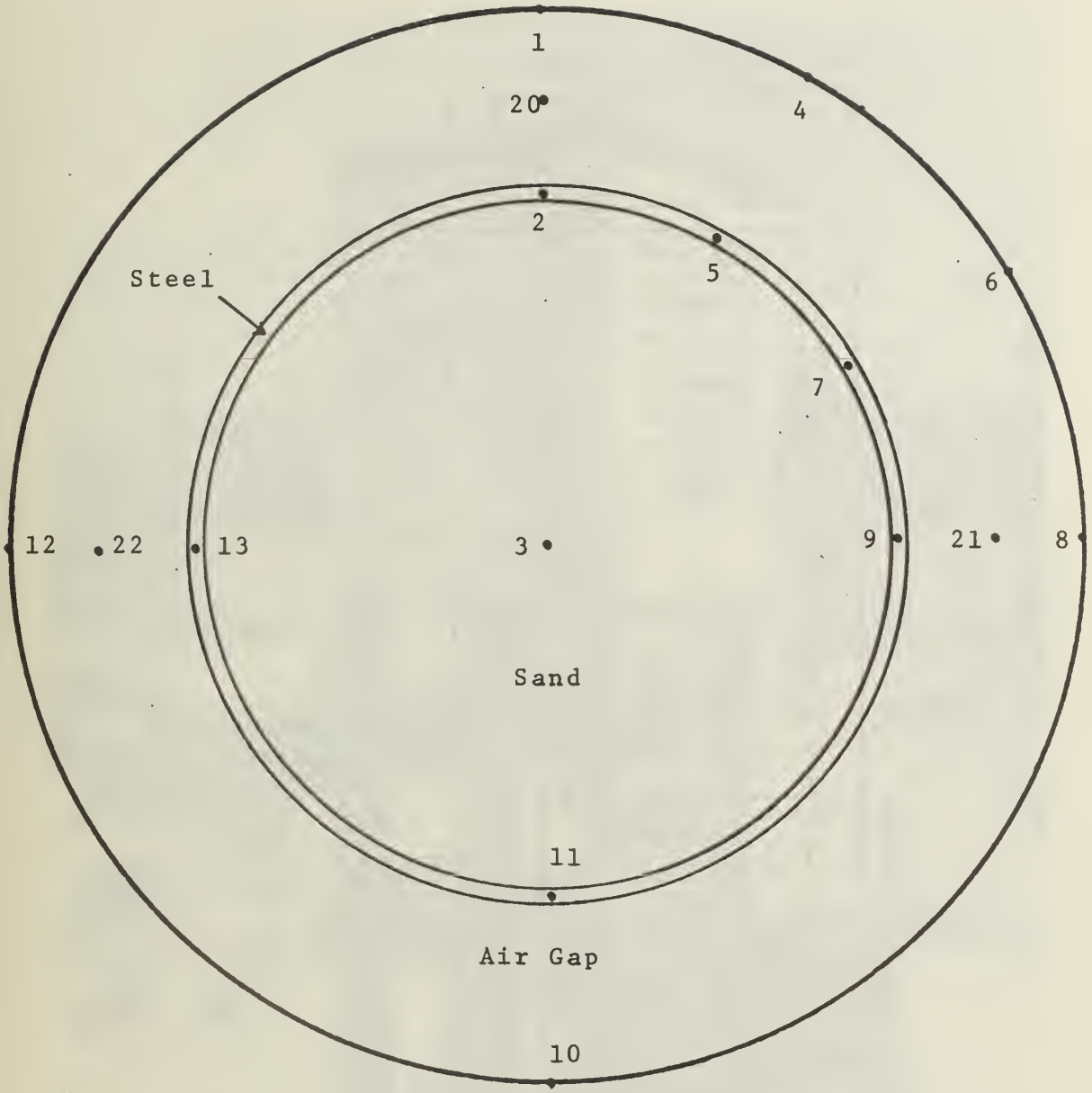

Figure 2. Thermocouple Locations on Experimental System.

Five thermocouples were located under the section painted with the liquid crystals. Their locations corresponding to the ones shown above are: #14= #1, #15= #2, #16= #8, #17= #9, and #18= #3 (See Figure 3).

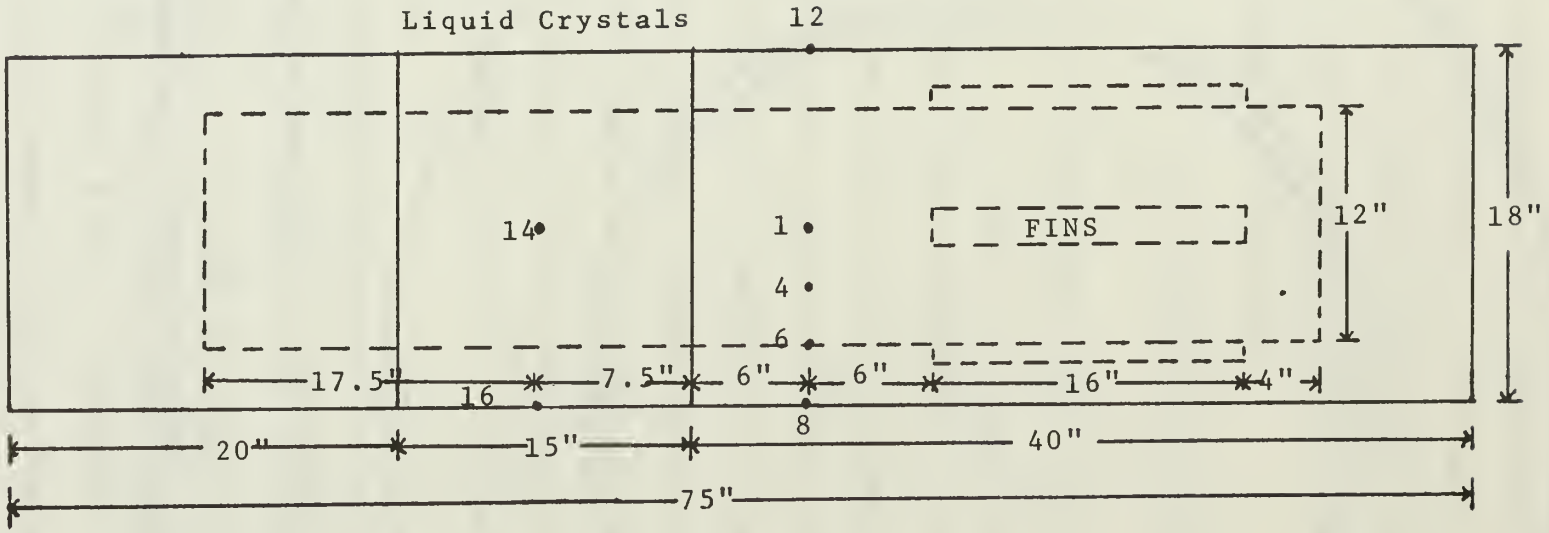

Figure 3. Top View of Rocket Motor Storage Container System.

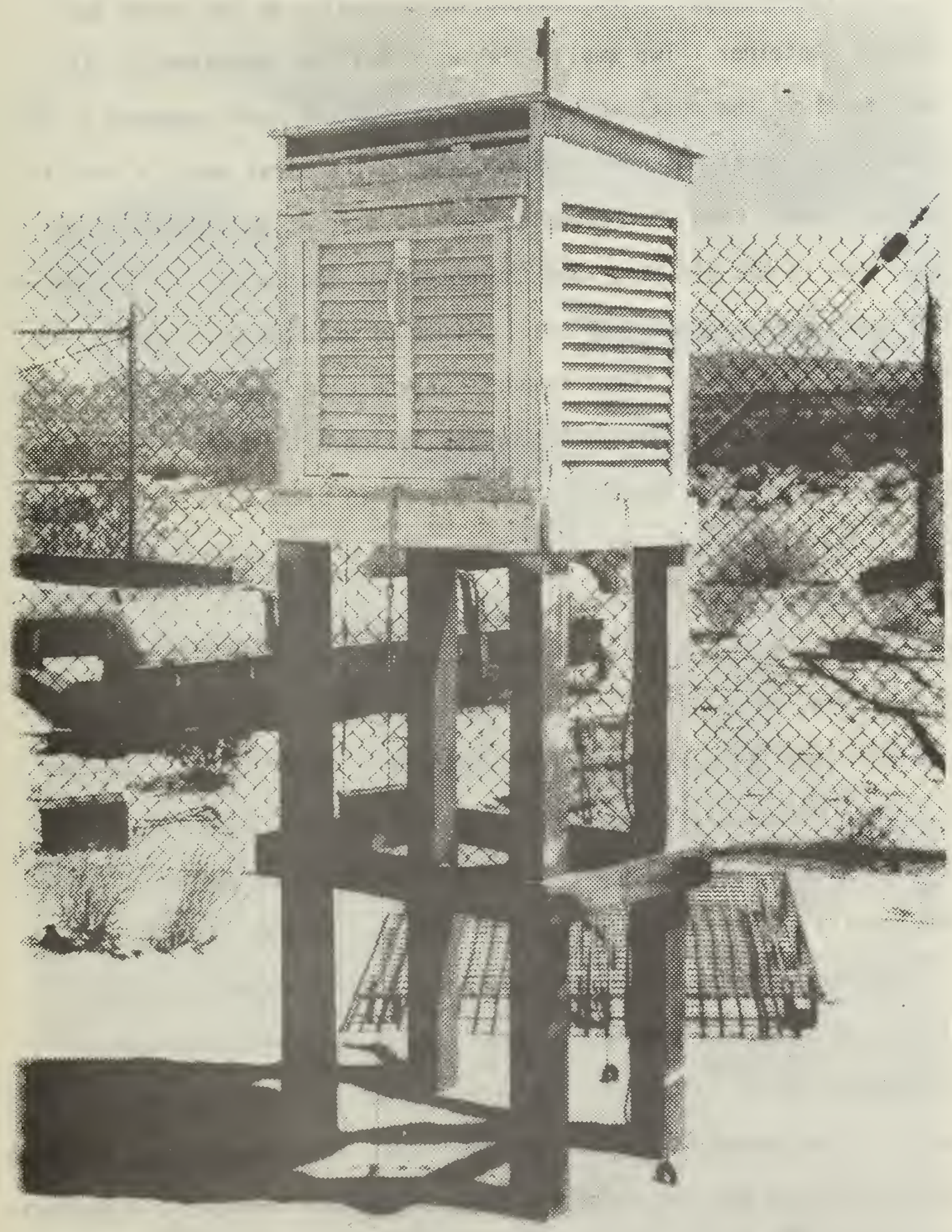

Figure 4. Stevenson Shelter.

The thermocouples were mounted intrinsically on the motor and storage container. Two small holes were drilled approximately 1/8 inch apart in the metal and the individual wires were inserted in the holes. The metal was then hammered around the wires until a snug fit was obtained. Bead thermocouples were mounted at the center of the motor and in the air gap. The thermocouples located at the center of the motor were supported by small pieces of wood several inches from the bead. The use of these supports was necessary to keep the thermocouples in position when the motor was filled with sand. After all the thermocouples on the rocket motor were in place, the rocket motor was filled with dry desert blown sand. The wires from the two thermocouples located in the center of the motor were led out a hole in the end cap. To avoid settling of the sand after the motor was in place on the site, with a resulting air gap being formed between the sand and the motor skin, the sand was compacted by striking the sides of the motor with small sledge hammers and then adding additional sand through the hole in the end cap. This was continued until the sand was tightly packed. The hole in the end cap was then sealed.

The rocket motor was carefully placed in its storage container (Figure 5) which had previously been instrumented with thermocouples. The thermocouples in the air gap were mounted by affixing the lead wire to the rocket motor at the desired position. A 90 degree bend was then put in the wire so that it placed the bead of the thermocouple approximately 1.5 inches into the air gap. Neither the thermocouples in the center of the motor nor those in the air gap could be considered accurately positioned. Every effort was made, however, to minimize positioning errors. All thermocouple wires were located inside the

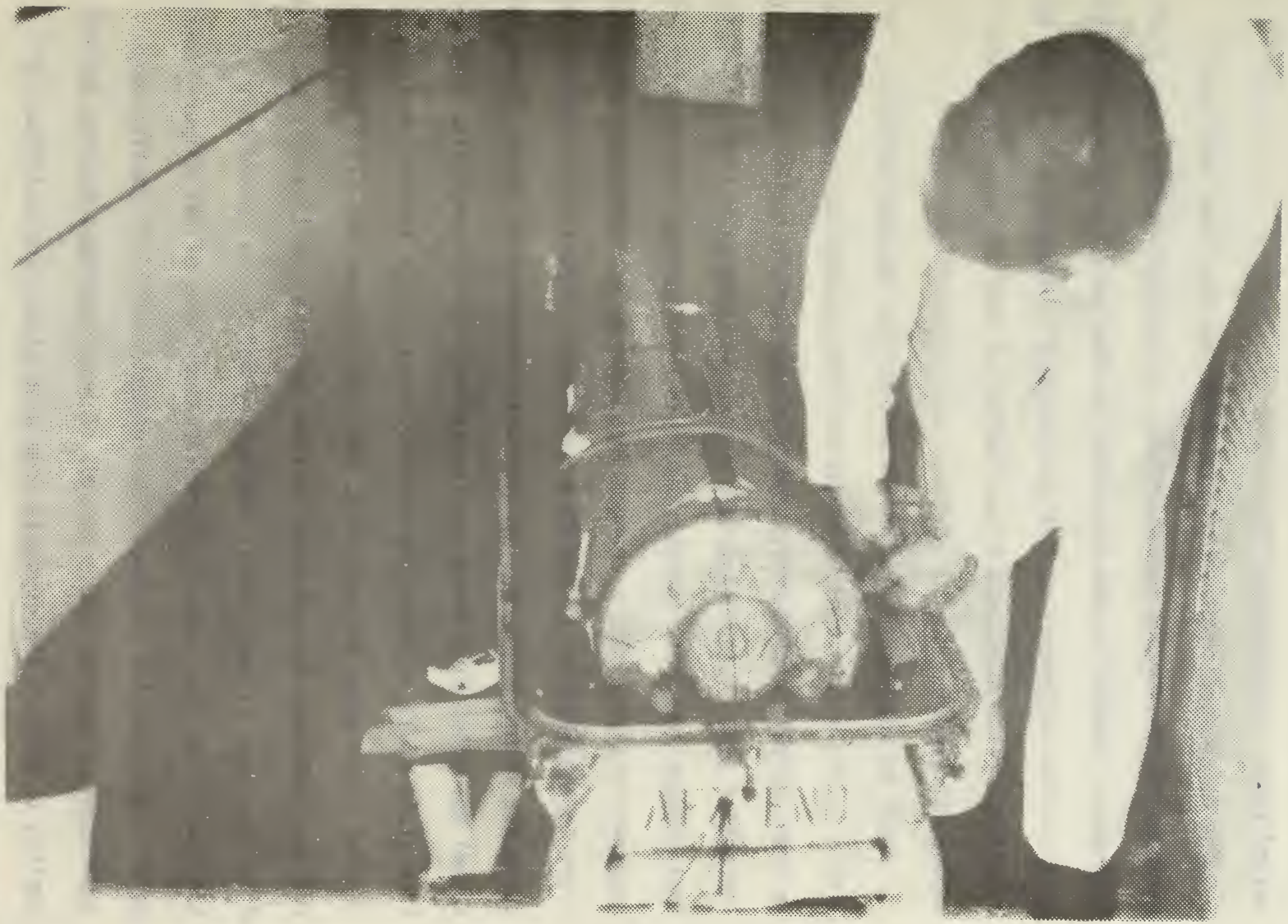

Figure 5. Rocket Motor Mounted in Storage Container.

storage container and were led through a hole in one end. This hole was then sealed. The two halves of the storage container were then bolted shut.

The outer surface of the rocket motor and the inner and outer surfaces of the storage container were all painted various shades of haze gray. Weathering had caused the painted surfaces to appear fairly rough. This is typical of the conditions of a storage dump. From the condition of the surfaces, it was estimated that the emissivity was approximately 0.9.

Prior to loading the rocket motor into the storage container, liquid crystals were applied to part of the storage container surface in order to obtain a thermal mapping of the surface temperature at any instant of time. Liquid crystals are temperature sensitive materials that produce immediate thermal images in a pattern of colors which respond rapidly to minute changes in substrate surface temperatures. Prior to applying the crystals, a 15 inch strip of the storage container, 20 inches from one end, was sprayed with two coats of Testors Spray Pla Enamel No. 1249, Flat Black as a background for the crystals. A one inch strip of 11 different ranges of crystal, with approximately 1/2 inch of black paint between them, was applied over the black paint. Two coats of each crystal were applied, using a small paint brush. The first coat was allowed to dry completely before the second coat was applied. After the crystals were dry, two coats of Rez polyurethane (gloss clear plastic coating, interior-exterior 77-5) coating were applied directly over the crystals. The polyurethane coating was applied to protect the crystals from wind blown sand and from the ultraviolet rays of the sun. Complete liquid crystal calibration

results are shown in Table 1. Details of the liquid crystal research will not be dwelt upon further in this report. The interested reader is referred to Reference 2 for additional information.

The rocket motor storage container system was then moved to the China Lake dump storage site. The system was aligned in a north-south direction, well away from the influence of other ordnance (Figure 6). The thermocouple leads were connected through a junction box and underground cable to a Honeywell Electronik 25 recorder which had been calibrated to read the thermocouple output directly in degrees Fahrenheit to an accuracy of ± 1°F. The recorder was located in an air-conditioned shed about 60 feet from the system.

Initial data indicated that thermocouple #7 was not responding properly, and, therefore, its output was neglected. Initial color photographs were taken of the liquid crystals, and it was immediately apparent that good thermal mappings could be obtained if the crystals were stable under the adverse desert environment. The brilliance of the colors exhibited by the crystals under the bright desert sun was much better than had been expected. The system was allowed two weeks to reach a periodic steady state before additional photographic data were obtained.

Extensive photographic data were collected on 27 and 28 July 1972 after two weeks of exposure to the desert environment. Both super 8 mm and 16 mm color movies and 35 mm color slides were taken of the liquid crystals. No colored filters were used on any of the cameras, although standard haze filters were used to take the super 8 mm movies and most of the 35 mm slides.

At this time a second storage container, this one without a rocket motor inside, was instrumented with intrinsic thermocouples in the same

TABLE I
Calibration of Liquid Crystals

NCR Desig.	Color Change	Manufacturer's Responses °C	Calibration Bath 2 Coats Liquid Crystals °C
R-27			
	Red	27.0	25.6±.5
	Green	28.6	28.0±.5
	Blue	30.0	28.7±.5
R-33			
	Red	33.0	32.7±.5
	Green	34.6	33.3±.5
	Blue	36.0	34.2±.5
R-37			
	Red	37.0	36.2±.5
	Green	38.6	37.1±.5
	Blue	40.0	38.0±.5
R-41			
	Red	41.0	40.3±.5
	Green	42.6	41.0±.5
	Blue	44.0	42.0±.5
R-45			
	Red	45.0	42.8±.5
	Green	46.6	43.6±.5
	Blue	48.0	44.3±.5
R-49			
	Red	49.0	46.7±.5
	Green	50.6	47.1±.5
	Blue	52.0	48.4±.5
R-53			
	Red	53.0	50.5±.5
	Green	54.6	52.1±.5
	Blue	56.0	53.3±.5
R-56			
	Red	56.0	53.8±.5
	Green	57.6	56.0±.5
	Blue	59.0	56.5±.5
R-59			
	Red	59.0	56.9±.5
	Green	60.6	57.5±.5
	Blue	62.0	58.9±.5
S-62			
	Red	62.0	60.1±.5
	Green	62.6	60.4±.5
	Blue	63.0	60.9±.5
S-64			
	Red	64.0	60.9±.5
	Green	64.6	61.4±.5
	Blue	65.0	62.7±.5

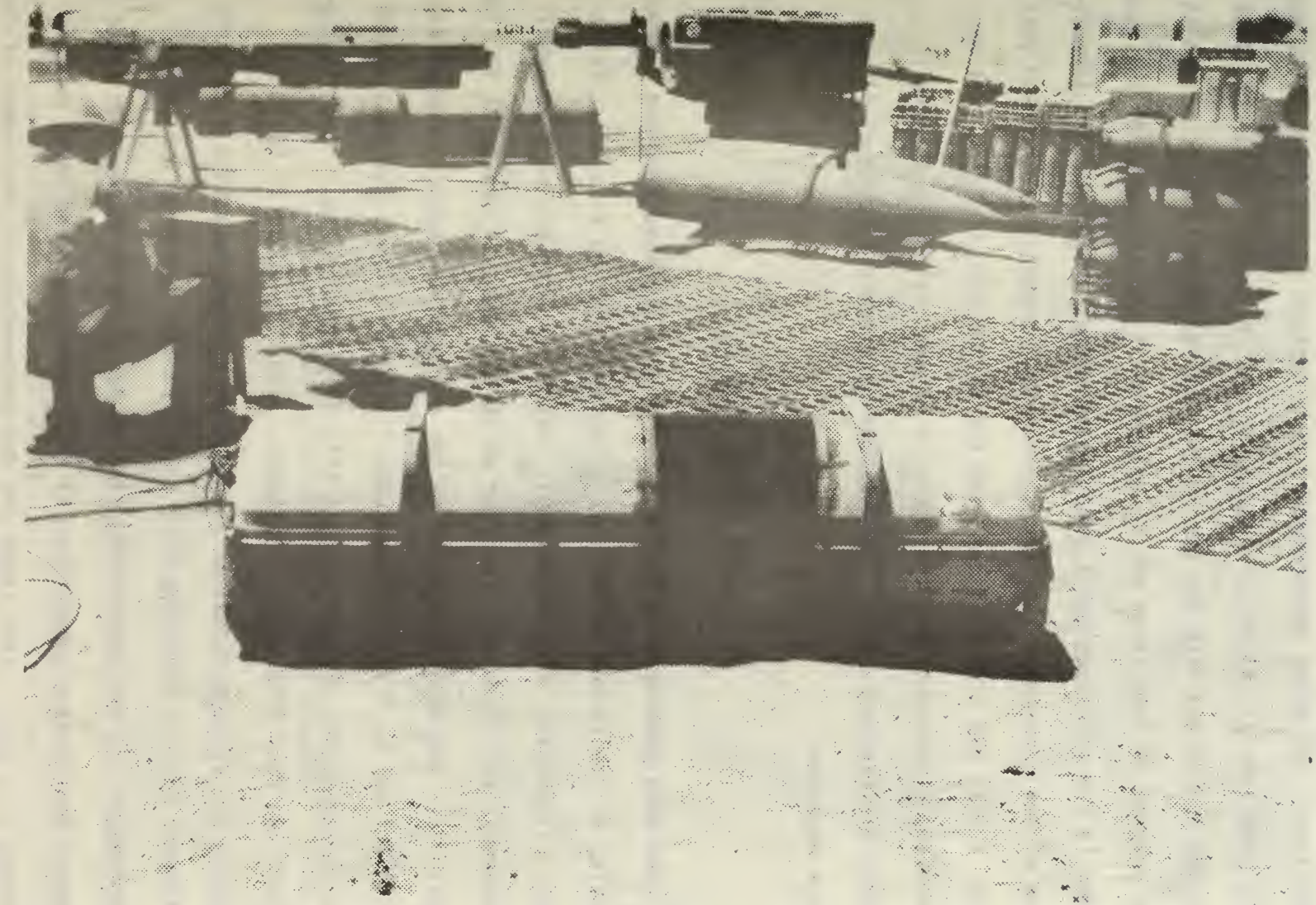

Figure 6. Experimental System at Dump Storage Site.

manner as the previous container. As only three data channels remained open on the recorder, only three thermocouples were applied to this new container. The three thermocouples were applied at the 0300, 0900, and 1200 positions at the axial midpoint of the container. This container was set end to end with the system that was already in place at the site. The purpose of this study was to determine if the inclusion of the rocket motor in the container had a significant effect on the surface temperature of the container. Thermocouple #7 was connected at the 0900 position, #23 at the 1200 position, and #24 at the 0300 position. It was immediately apparent that thermocouple #7 was continuing to give unreliable readings, and therefore, the data taken on channel #7 were again neglected.

IV. EXPERIMENTAL RESULTS

The data presented in Tables 2 and 3 were obtained from the thermocouples on the rocket motor storage container system located at China Lake, California. The thermocouple output was read out on a Honeywell Electronik 25, 24 channel recorder which had been calibrated at 50, 100, and 150°F. The data were taken on two consecutive, typical summer days (August 1 and 2, 1972) at China Lake. (Figure 7 shows the location of the thermocouples used to collect this temperature data.) Each thermocouple was read once every 24 minutes. The data shown in Table 2 present the storage container temperature at four locations plus three different ways of averaging this data. It also presents the ambient temperature and the approximate time of day. The data shown in Table 3 present the surface temperature of the rocket motor and three ways to average this data. Also shown are the temperature at the center of the rocket motor and the approximate time of day.

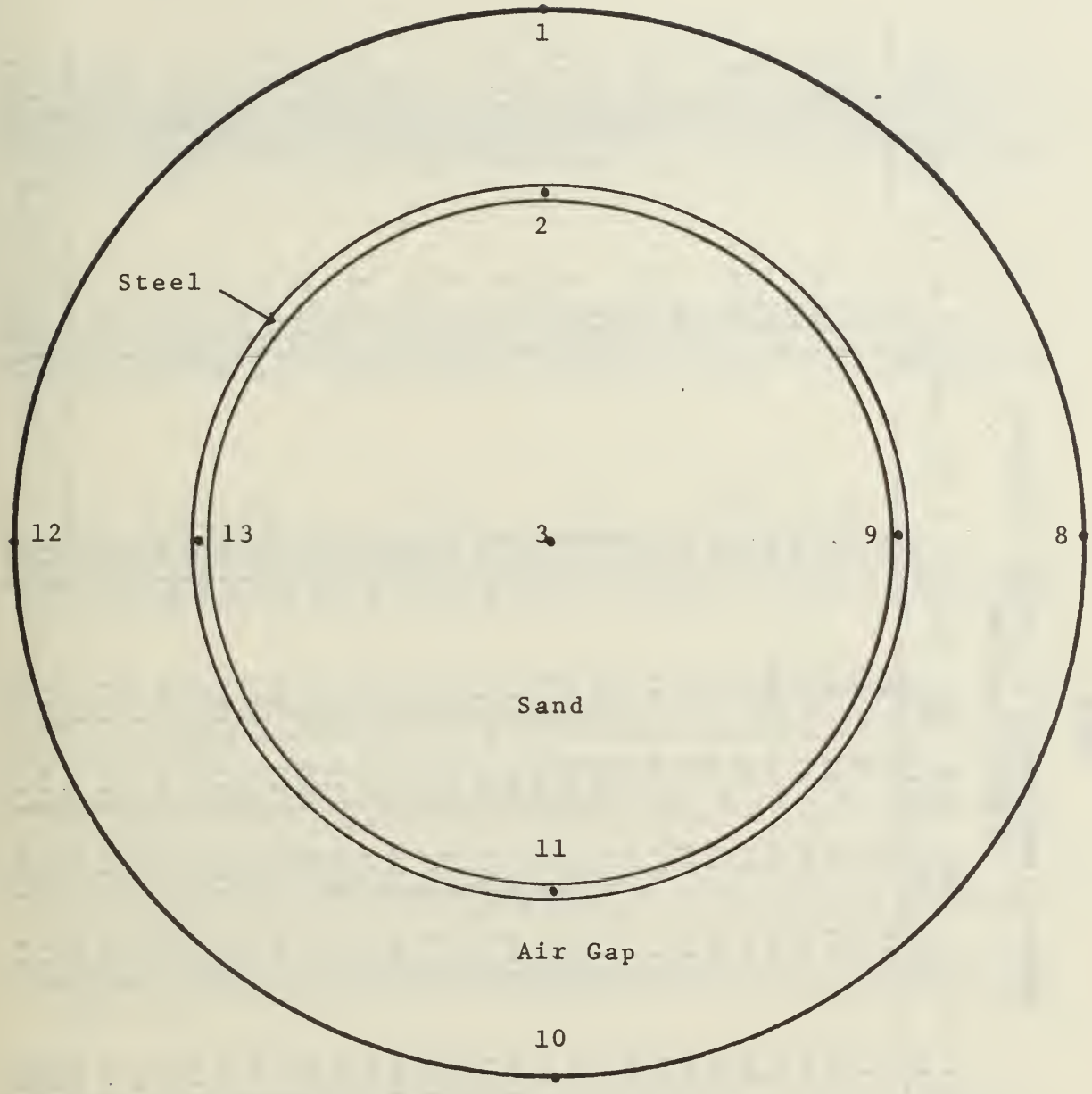

Figure 7: Thermocouple Locations for Experimental Data.

TABLE 2

Measured Temperatures at Various Locations
on ASROC container

Time (Approximate) Aug. 1, 1972	Ambient (°F)	#1 (°F)	#8 (°F)	#10 (°F)	#12 (°F)	Avg.#1 & #10 (°F)	Avg.#8 & #12 (°F)	Avg. all 4 "Bulk"
0536	76	69	72	79	80	74	76	75
0600	77	68	72	79	80	73.5	76	74.75
0624	80	73	75	81	82	77	78.5	77.75
0648	80	81	79	87	85	84	82	83
0712	83	90	82	90	89	90	85.5	87.75
0736	85	98	87	93	92	95.5	89.5	92.5
0800	87	105	90	94	94	99.5	92	95.75
	89	110	93	96	97	103	95	99
	91	116	96	98	99	107	97.5	102.25
	92	121	100	101	102	111	101	106
	94	129	103	102	105	115.5	104	109.75
1000	96	133	107	105	108	119	107.5	113.25
	97	139	110	107	110	123	110	116.5
	100	143	113	107	112	125	112.5	118.75
	101	147	117	109	115	128	116	122
	103	150	119	109	116	129.5	117.5	123.5
1200	104	153	124	110	119	131.5	121.5	126.5
	106	156	128	112	122	134	125	129.5
	106	157	131	113	124	135	127.5	131.25
	106	154	133	114	125	134	129	131.5
	107	157	138	115	127	136	132.5	134.25
1400	108	154	143	117	129	135.5	136	135.75
	109	153	142	118	129	135.5	135.5	135.5
	110	148	142	119	129	133.5	135.5	134.5
	110	143	141	118	128	130.5	134.5	132.5
	109	142	143	119	128	130.5	135.5	133
1600	107	137	143	119	128	128	135.5	131.75
	108	134	139	117	127	125.5	133	129.25
	108	130	139	117	127	123.5	133	128.25
	106	126	138	116	126	121	132	126.5
	104	123	136	115	125	119	130.5	124.75

TABLE 2 (Continued)

Time (Approximate) Aug. 1, 1972	Ambient (°F)	#1 (°F)	#8 (°F)	#10 (°F)	#12 (°F)	Avg. #1 & #10 (°F)	Avg. #8 & #12 (°F)	Avg. all 4 "Bulk
1800	103	118	131	113	123	115.5	127	121.25
	101	113	127	111	120	112	123.5	117.75
	99	107	121	108	117	107.5	119	113.25
	96	101	106	103	111	102	108.5	105.25
	95	91	93	98	104	94.5	98.5	96.5
2000	93	88	91	95	101	91.5	96	93.75
	91	86	89	94	99	90	94	92
	90	85	88	92	97	88.5	92.5	90.5
	89	84	87	91	96	87.5	91.5	89.5
	87	83	85	89	94	86	89.5	87.75
2200	87	81	84	88	93	84.5	88.5	86.5
	85	80	83	87	91	83.5	87	85.25
	86	79	82	86	91	82.5	86.5	84.5
	86	79	82	87	90	83	86	84.5
	84	79	82	86	89	82.5	85.5	84
0000 2 Aug.	82	77	80	85	88	81	84	82.5
	81	74	78	84	86	79	82	80.5
	81	72	76	83	85	77.5	80.5	79
	81	72	77	83	85	77.5	81	79.25
	79	72	75	81	83	76.5	79	77.75
0200	79	72	75	80	83	76	79	77.5
	79	72	74	80	82	76	78	77
	78	72	74	79	82	75.5	78	76.75
	77	71	73	79	81	75	77	76
	75	70	72	78	80	74	76	75
0400	73	67	69	77	78	72	73.5	72.75
	72	66	69	75	77	70.5	73	71.75
	73	65	68	75	76	70	72	71
	69	64	67	73	75	68.5	71	69.75
	69	63	66	72	74	67.5	70	68.75
0600	68	63	66	71	73	67	69.5	68.25
	71	65	67	75	76	70	71.5	70.75
	77	74	71	80	79	77	75	76
	79	84	77	84	84	84	80.5	82.25

TABLE 2 (Continued)

Time (Approximate) Aug. 2, 1972	Ambient (°F)	#1 (°F)	#8 (°F)	#10 (°F)	#12 (°F)	Avg. #1 & #10 (°F)	Avg. #8 & #12 (°F)	Avg. all 4 "Bulk"
	80	93	81	89	87	91	84	87.5
0800	83	101	85	92	91	96.5	88	92.25
	85	108	89	93	93	100.5	91	95.75
	86	114	93	96	97	105	95	100
	88	121	96	98	100	109.5	98	103.75
	89	126	98	98	101	112	99.5	105.75
1000	91	130	101	100	103	115	102	108.5
	94	137	106	102	106	119.5	106	112.75
	96	143	109	104	109	123.5	109	116.25
	100	146	113	106	111	126	112	119
	100	149	117	107	114	128	115.5	121.75
1200	101	151	121	108	117	129.5	119	124.25
	103	150	127	110	119	130	123	126.5
	104	156	129	110	121	133	125	129
	104	154	133	111	122	132.5	127.5	130
	105	155	137	112	125	133.5	131	132.25
1400	105	156	141	114	126	135	133.5	134.25
	107	149	143	114	127	131.5	135	133.25
	107	149	146	115	128	132	137	134.5
	106	151	152	118	131	134.5	141.5	138
	107	144	152	120	132	132	142	137
1600	108	139	152	119	131	129	141.5	135.25
	107	136	147	120	130	128	138.5	133.25
	107	136	147	121	130	128.5	138.5	133.5
	105	131	147	121	130	126	138.5	132.25
	103	124	144	120	128	122	136	129
1800	103	117	134	117	124	117	129	123
	100	111	119	113	121	112	120	116
	98	105	118	108	117	106.5	117.5	112
	95	99	103	103	109	101	106	103.5
	93	91	93	97	103	94	98	96
2000	91	87	90	94	100	90.5	95	92.75
	90	85	88	93	98	89	93	91
	88	83	86	91	96	87	91	89

TABLE 2 (Continued)

Time (Approximate) Aug. 2, 1972	Ambient (°F)	#1 (°F)	#8 (°F)	#10 (°F)	#12 (°F)	Avg. #1 & #10 (°F)	Avg. #8 & #12 (°F)	Avg. all 4 "Bulk"
	87	81	85	90	94	85.5	89.5	87.5
	85	80	83	88	93	84	88	86
2200	84	78	81	87	91	82.5	86	84.25
	82	75	78	86	89	80.5	83.5	82
	85	74	79	85	88	79.5	83.5	81.5
	83	76	78	85	87	80.5	82.5	81.5
	81	74	77	84	86	79	81.5	80.25
0000 3 Aug.	78	71	75	83	84	77	79.5	78.25
	81	69	74	81	84	75	79	77
	79	70	73	81	83	75.5	78	76.75
	79	72	74	80	83	76	78.5	77.25
	78	71	73	79	82	75	77.5	76.25
0200	77	70	72	78	81	74	76.5	75.25
	73	69	71	77	79	73	75	74
	72	65	69	76	78	70.5	73.5	72
	70	64	68	74	77	69	72.5	70.75
	67	63	66	73	75	68	70.5	69.25
0400	67	61	65	71	74	66	69.5	67.75
	66	60	64	70	73	65	68.5	66.75
	65	60	63	70	72	65	67.5	66.25
	65	58	61	69	71	63.5	66	64.75
			FIRST DAY'S TEMPERATURE RANGES					
HIGH	110	157	143	119	129	136	136	135.75
LOW	69	64	67	73	75	68.5	71	69.75
AVG	89.5	110.5	105	96	102	102.25	103.5	102.75
			SECOND DAY'S TEMPERATURE RANGES					
HIGH	108	156	152	121	132	135	142	138
LOW	65	58	61	69	71	63.5	66	64.75
AVG	86.5	107	106.5	95	101.5	99.25	104	101.38

TABLE 3

Measured Temperatures at Various Locations on the Surface and in the Center of a Sand-filled ASROC Motor

Time (Approximate) Aug. 1, 1972	#3 (°F)	#2 (°F)	#9 (°F)	#11 (°F)	#13 (°F)	Avg. #2 & #11 (°F)	Avg. #9 & #13 (°F)	Avg. all 4 (°F)
0536	97	83	84	85	85	84	84.5	84.25
0600	96	82	83	85	84	83.5	83.5	83.5
0624	95	82	83	84	85	83	84	83.5
0648	94	85	84	86	89	85.5	86.5	86
0712	94	88	86	88	93	88	89.5	88.75
0736	93	91	88	90	96	90.5	92	91.25
0800	92	95	90	91	99	93	94.5	93.75
	91	98	92	93	102	95.5	97	96.25
	91	101	94	95	104	98	99	98.5
	91	105	96	97	107	101	101.5	101.25
	91	108	98	98	109	103	103.5	103.25
1000	91	112	101	100	112	106	106.5	106.25
	91	115	103	102	113	108.5	108	108.25
	92	118	105	103	115	110.5	110	110.25
	94	120	108	105	117	112.5	112.5	112.5
	94	122	110	106	118	114	114	114
1200	95	125	111	108	119	116.5	115	115.75
	96	126	114	109	120	117.5	117	117.25
	98	128	117	111	121	119.5	119	119.25
	100	130	119	112	122	121	120.5	120.75
	101	130	120	113	122	121.5	121	121.25
1400	102	131	122	114	122	122.5	122	122.25
	103	131	123	115	121	123	122	122.5
	105	131	124	117	121	124	122.5	123.25
	107	129	125	117	121	123	123	123
	108	129	125	118	120	123.5	122.5	123
1600	109	127	125	117	119	122	122	122
	111	126	125	117	119	121.5	122	121.75
	112	125	125	118	118	121.5	121.5	121.5
	113	124	125	118	117	121	121	121
	114	123	124	117	116	120	120	120

TABLE 3 (Continued)

Time (Approximate) Aug. 1, 1972	#3 (°F)	#2 (°F)	#9 (°F)	#11 (°F)	#13 (°F)	Avg.#2 & #11 (°F)	Avg.#9 & #13 (°F)	Avg.all 4 (°F)
1800	115	121	123	117	115	119	119	119
	115	119	121	115	113	117	117	117
	116	117	119	114	112	115.5	115.5	115.5
	117	115	116	112	111	113.5	113.5	113.5
	117	111	111	109	108	110	109.5	109.75
2000	117	107	107	106	106	106.5	106.5	106.5
	117	105	105	104	104	104.5	104.5	104.5
	116	103	103	103	102	103	102.5	102.75
	116	101	101	101	101	101	101	101
	115	100	100	100	100	100	100	100
2200	114	98	98	98	98	98	98	98
	113	97	97	97	97	97	97	97
	112	95	95	96	95	95.5	95	95.25
	111	94	95	95	95	94.5	95	94.75
	110	93	94	94	94	93.5	94	93.75
0000 2 Aug.	109	92	93	93	93	92.5	93	92.75
	107	91	91	92	92	91.5	91.5	91.5
	106	89	90	91	90	90	90	90
	105	88	89	90	89	89	89	89
	104	87	88	89	89	88	88.5	88.25
0200	103	87	87	88	88	87.5	87.5	87.5
	102	86	86	87	87	86.5	86.5	86.5
	101	85	86	87	86	86	86	86
	100	84	85	86	85	85	85	85
	99	83	84	85	85	84	84.5	84.25
0400	97	82	83	84	83	83	83	83
	96	81	82	83	82	82	82	82
	95	80	80	82	81	81	80.5	80.25
	94	79	80	81	80	80	80	80
	93	78	79	80	79	79	79	79
0600	92	77	78	79	78	78	78	78
	91	76	77	79	80	77.5	78.5	78
	90	79	78	80	84	79.5	81	80.25
	89	82	80	82	88	82	84	83

TABLE 3 (Continued)

Time (Approximate) Aug. 2, 1972	#3 (°F)	#2 (°F)	#9 (°F)	#11 (°F)	#13 (°F)	Avg. #2 & #11 (°F)	Avg. #9 & #13 (°F)	Avg. all 4 (°F)
	88	87	82	85	92	86	87	86.5
0800	87	90	85	87	96	88.5	90.5	89.5
	86	95	87	89	99	92	93	92.5
	86	98	90	91	102	94.5	96	95.25
	86	102	92	93	105	97.5	98.5	98
	86	106	95	95	107	100.5	101	100.75
1000	87	108	97	96	108	102	102.5	102.25
	87	111	99	98	110	104.5	104.5	104.5
	88	115	102	100	113	107.5	107.5	107.5
	89	118	104	101	114	109.5	109	109.25
	90	120	107	103	115	111.5	111	111.25
1200,	91	122	109	105	116	113.5	112.5	113
	92	123	111	107	117	115	114	114.5
	94	125	114	108	117	116.5	115.5	116
	95	127	116	109	118	118	117	117.5
	97	127	118	110	118	118.5	118	118.25
1400	98	128	120	111	119	119.5	119.5	119.5
	100	128	121	112	118	120	119.5	119.75
	102	128	122	113	118	120.5	120	120.25
	103	129	125	115	118	122	121.5	121.75
	105	129	126	116	118	122.5	122	122.25
1600	106	128	127	116	118	122	122.5	122.25
	107	127	127	117	117	122	122	122
	109	127	128	119	118	123	123	123
	110	126	128	119	117	122.5	122.5	122.5
	111	124	127	118	116	121	121.5	121.25
1800	112	122	125	117	115	119.5	120	119.75
	114	120	123	117	113	118.5	118	118.25
	114	117	120	114	112	115.5	116	115.75
	115	114	116	112	110	113	113	113
	116	110	110	108	107	109	108.5	108.75
2000	116	107	107	106	105	106.5	106	106.25
	117	104	104	103	103	103.5	103.5	103.5
	116	102	102	102	101	102	101.5	101.75

TABLE 3 (Continued)

Time (Approximate) Aug. 2, 1972	#3 (°F)	#2 (°F)	#9 (°F)	#11 (°F)	#13 (°F)	Avg.#2 & #11 (°F)	Avg.#9 & #13 (°F)	Avg.all 4 (°F)
	115	100	100	100	100	100	100	100
	114	98	99	99	98	98.5	98.5	98.5
2200	113	96	97	97	96	96.5	96.5	96.5
	112	95	95	96	95	95.5	95	95.25
	111	93	94	94	93	93.5	93.5	93.5
	110	92	93	93	93	92.5	93	92.75
	109	91	91	92	91	91.5	91	91.25
0000 3 Aug.	108	89	90	91	90	90	90	90
	106	88	89	90	89	89	89	89
	105	87	88	89	88	88	88	88
	104	86	87	88	87	87	87	87
	103	85	86	87	87	86	86.5	86.25
0200	101	85	85	86	86	85.5	85.5	85.5
	100	84	84	85	85	84.5	84.5	84.5
	99	82	83	84	83	83	83	83
	98	81	82	83	82	82	82	82
	97	80	80	81	81	80.5	80.5	80.5
0400	95	78	79	80	79	79	79	79
0424	94	77	78	79	78	78	78	78
0448	93	76	77	78	77	77	77	77
0512	92	75	76	77	76	76	76	76
FIRST DAY'S TEMPERATURE RANGES								
HIGH	117	131	125	118	122	124	123	123.25
LOW	91	79	80	81	80	80	80	80
AVG	104	105	102.5	99.5	101	102	101.5	101.63
SECOND DAY'S TEMPERATURE RANGES								
HIGH	116	129	128	119	119	122.5	122.5	122.5
LOW	86	75	76	77	76	76	76	76
AVG	101	102	102	98	97.5	99.25	99.25	99.25

Table 4 compares the temperatures measured at the 12 o'clock location on the empty container with those measured on the container which contained the ASROC motor. For convenience, in the same table, the bulk container temperature has been compared with the average of the 12 o'clock temperature and the ambient temperature. The reason for presenting this information is discussed under Conclusions and Recommendations.

V. THEORETICAL ANALYSIS

A. Introductory Remarks

In the present analytical investigation the container surface temperature variation was assumed known a priori. The results of our experimental investigation indicate that there is a significant temperature variation, as much as 45°F, around the circumference of the container. The heat transferred to the rocket motor stored inside the container arrives by the combined effects of thermal radiation and convection across the air gap separating the motor and the container. The air gap represents a significant thermal resistance to the heat transfer process and, further, tends to smooth the spatial temperature variation around the circumference of the motor. This may be seen by examining the experimental data, Table 4, and noting that the motor circumferential temperature variation is a maximum of 18°F, and this only occurs for a short time span each day. Accordingly, it seemed reasonable to assume that within the rocket motor, heat transfer would be essentially one-dimensional, with the primary direction being radial. In order to develop a one-dimensional analytical solution, the container circumferential temperature variation was averaged to develop a

TABLE 4

Comparison of Measured Temperatures on two ASROC containers: One container contained a sand-filled motor, and the second container was empty

Time	Ambient	Top, Filled Container	Top, Empty Container	Average Air&Contain.	Actual Bulk
Aug.1,1972	(°F)	(°F)	(°F)	(°F)	(°F)
0536	76	69	67	73	75
0600	77	68	66	73	75
0624	80	73	70	77	78
0648	80	81	79	81	83
0712	83	90	88	87	88
0736	85	98	98	92	92
0800	87	105	105	96	96
	89	110	110	99	99
	91	116	116	104	102
	92	121	121	107	106
	94	129	128	111	110
1000	96	133	133	114	113
	97	139	139	118	116
	100	143	143	121	119
	101	147	146	124	122
	103	150	147	126	124
1200	104	153	150	128	126
	106	156	152	131	130
	106	157	152	131	131
	106	154	150	130	132
	107	157	150	132	134
1400	108	154	150	131	136
	109	153	149	131	136
	110	148	145	129	134
	110	143	138	127	133
	109	142	137	126	133

TABLE 4 (Continued)

Time	Ambient	Top, Filled Container	Top, Empty Container	Average Air&Contain.	Actual Bulk
Aug.1,1972) cont'd.)					
1600					
	107	137	133	122	132
	108	134	130	121	129
	108	130	126	119	128
	106	126	121	116	126
	104	123	120	114	125
1800	103	118	114	111	121
	101	113	109	107	118
	99	107	104	103	113
	96	101	99	98	105
	95	91	88	93	96
2000	93	88	84	91	94
	91	86	82	89	92
	90	85	82	88	91
	89	84	80	87	90
	87	83	79	85	88
2200	87	81	78	84	86
	85	80	77	82	85
	86	79	76	82	84
	86	79	76	82	84
	84	79	76	81	84
2 Aug 0000	82	77	74	79	82
	81	74	70	77	80
	81	72	67	76	79
	81	72	67	76	79
	79	72	68	75	78
0200	79	72	68	75	78
	79	72	68	75	77
	78	72	68	75	77
	77	71	67	74	76
	75	70	66	72	75

TABLE 4 (Continued)

Time	Ambient	Top, Filled Container	Top, Empty Container	Average Air&Contain.	Actual Bulk
Aug.2,1972) cont'd.)					
0400	73	67	63	70	73
	72	66	61	69	72
	73	65	61	69	71
	69	64	60	67	70
	69	63	58	66	69
0600	68	63	58	65	68
	71	65	59	68	71
	77	74	70	76	76
	79	84	83	82	82
	80	93	92	87	88
0800	83	101	99	91	92
	85	108	108	96	96
	86	114	114	100	100
	88	121	121	104	104
	89	126	126	107	106
1000	91	130	129	109	108
	94	137	135	115	113
	96	143	141	119	116
	100	146	144	123	119
	100	149	147	124	122
1200	101	151	148	126	124
	103	150	147	127	126
	104	156	150	130	129
	104	154	149	129	130
	105	155	147	130	132
1400	105	156	149	131	134
	107	149	142	128	133
	107	149	142	128	134
	106	151	143	129	138
	107	144	138	126	137
1600	108	139	134	124	135
	107	136	132	122	133

TABLE 4 (Continued)

Time	Ambient	Top, Filled Container	Top, Empty Container	Average Air&Contain.	Actual Bulk
Aug.2,1972) cont'd.)					
	107	136	130	122	133
	105	131	126	116	132
	103	124	118	114	129
1800	103	117	113	110	123
	100	111	109	106	116
	98	105	102	102	112
	95	99	96	97	103
	93	91	88	92	96
2000	91	87	84	89	93
	90	85	82	87	91
	88	83	80	86	89
	87	81	77	84	87
	85	80	75	82	86
2200	84	78	72	81	84
	82	75	71	79	82
	85	74	67	79	81
	83	76	70	79	81
	81	74	69	77	80
3 Aug. 0000	78	71	66	75	78
	81	69	62	75	77
	79	70	66	75	77
	79	72	70	75	77
	78	71	67	74	76
0200	77	70	66	73	75
	73	69	66	71	74
	72	65	60	69	72
	70	64	59	67	71
	67	63	57	65	69
0400	67	61	56	64	68
	66	60	55	63	67
	65	60	54	63	66

TABLE 4 (Continued)

Time	Ambient	Top, Filled Container	Top, Empty Container	Average Air&Contain.	Actual Bulk
Aug.3,1972) cont'd.)					
	65	58	52	61	65
	65	58	51	61	64
0600	65	58	52	61	64

relationship between the container bulk temperature and time. By definition:

$$T_{bulk} = \frac{\int c_p T dV}{\int c_p dV} \tag{1}$$

where

T = container temperature

c_p = container specific heat

dV = container elemental volume

Noting that the specific heat of steel, c_p, is essentially constant over the temperature range of interest and that the elemental volume, dV, is directly proportional to the elemental angular increment, $d\gamma$, Equation (1) reduces to:

$$T_{bulk} = \frac{1}{2\pi} \int_0^{2\pi} T \, d\gamma \tag{2}$$

Since container surface temperature data were available only at discrete locations around the circumference, equation (2) was approximated as:

$$T_{bulk} \approx \frac{1}{2\pi} \sum_{i=1}^{4} T_i \left(\frac{\pi}{2}\right) \tag{3}$$

$$\approx \frac{1}{4} \sum_{i=1}^{4} T_i$$

where the T_i's are the measured temperatures at the 12, 3, 6, and 9 o'clock positions on the container.

Equation (3) was used to convert local experimental data to bulk temperature information. Figure 8 shows the bulk temperature variation as a function of time as experimentally recorded on 2 August 1972. Shown as a continuous curve on the same graph is a pure sine wave with the same period and amplitude. While the agreement is not perfect, note that over a significant portion of the transient, the agreement is quite close. Due to this agreement it was decided to model the container bulk temperature-time variation as a pure sine wave of the form:

$$T_c = (T_m - T_a) \sin \omega t + T_a \qquad (4)$$

where

T_c = container bulk temperature

T_m = maximum bulk temperature

T_a = average bulk temperature

t = time

ω = circular frequency (2π/period)

B. One-dimensional Analytical Model

The method of complex temperatures, as presented by Arpaci [1], was used to find the radial temperature distribution in a cylindrical rocket motor stored in a cylindrical container. The container temperature was assumed to vary in the form given by Equation (4). The complete analytical derivation may be found in reference 2. The major assumptions employed in the model are: heat flow is one dimensional in the radial direction only, no heat sources or sinks exist within the motor, and

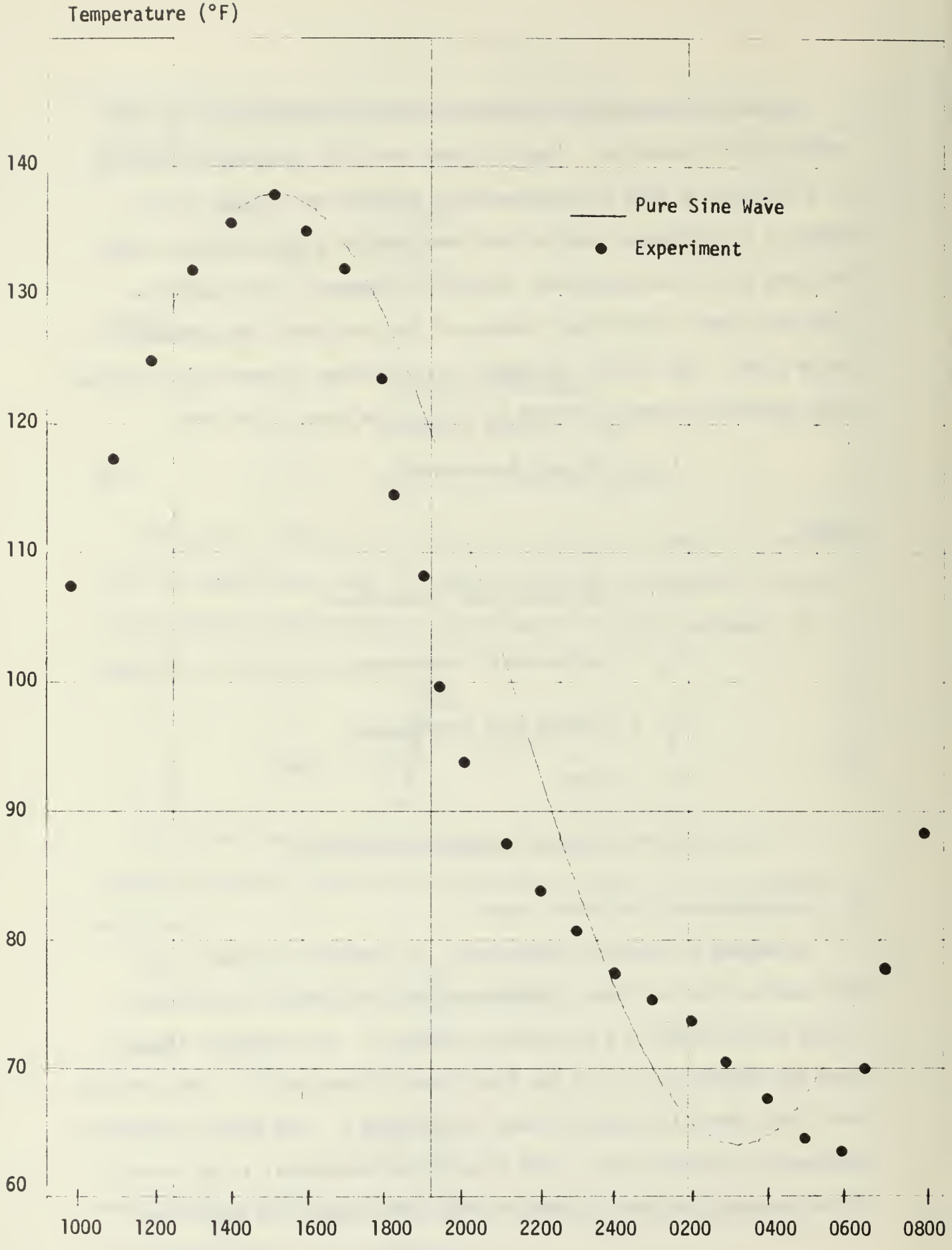

Figure 8. Comparison of Pure Sinusoidal Temperature Variation with Measured Container Bulk Temperature.

the sinusoidally varying surface temperature is spacially uniform over the entire container surface.

Heat transfer across the air gap was treated by employing the concept of an overall gap conductance, $\bar{h}$. This overall conductance combines the effects of both radiation and convection. Assuming that the radiation and convection processes are uncoupled, one may write:

$$\bar{h} = h_r + h_c \tag{5}$$

where

h_r = linearized gap radiation coefficient

h_c = gap convective coefficient

The net heat transfer rate between the motor and container is:

$$Q_{1-2} = \bar{h} A_1 (T_1 - T_2) \tag{6}$$

where

Q_{1-2} = heat transfer rate between motor and container

A_1 = motor surface area

T_1 = motor bulk surface temperature

T_2 = container bulk surface temperature

The gap radiation coefficient, h_r, was found by linearizing the grey body radiation relationship:

$$Q_{r_{1-2}} = F_{1-2}\,\sigma\,A_1\,(T_1^4 - T_2^4)$$

$$= F_{1-2}\,\sigma\,(T_1 + T_2)\,(T_1^2 + T_2^2)\,A_1\,(T_1 - T_2) \qquad (7)$$

$$= h_r A_1\,(T_1 - T_2)$$

where

$$h_r = F_{1-2}\,\sigma\,(T_1 + T_2)\,(T_1^2 + T_2^2) \qquad (8)$$

and

F_{1-2} = Grey body exchange factor

σ = Stefan-Boltzmann constant

T_1 = Motor skin temperature

T_2 = Container temperature

The gap convective coefficient, h_c, may be found by using the correlations developed by Liu, Mueller, and Landis [3] for convection across cylindrical gaps, namely:

$$h_c = \frac{\left[0.135 k_g\right]}{\left[r_1 \ln {}^{r_2}/_{r_1}\right]} \frac{\left[P_r^2 Gr\right]^{(0.278)}}{\left[1.36 + Pr\right]} \qquad (9)$$

where

k_g = Thermal conductivity of the gas in the gap

Pr = Prandtl number = ν/α

ν = Gas kinematic viscosity

α = Gas thermal diffusivity

Gr = Grashof number = $\frac{g\beta\Delta T\Delta r^3}{\nu^2}$

g = Local gravity acceleration

β = Thermal coefficient of expansion

ΔT = $(T_1 - T_2)$

Δr = $(r_2 - r_1)$

r_1 = motor radius

r_2 = container radius

The steady, periodic solution describing the radial temperature distribution in the rocket motor, T(r,t), is developed in detail in Reference 2 using the method of complex temperatures [1]. The solution, in normalized form, is:

$$\frac{(T(r,t) - T_a)}{(T_m - T_a)} = \frac{\left[ber_o^2(A\xi) + bei_o^2(A\xi)\right]^{1/2}}{\left[X_r^2 + X_i^2\right]^{1/2}} \sin(\omega t + \delta) \quad (10)$$

or

$$\theta(r, t) = \theta_r \sin(\omega t + \delta) \quad (11)$$

where

T(r,t) = Motor temperature at radial location r and time t

T_a = Average container temperature

T_m = Maximum container temperature

$\theta(r,t)$ = Normalized temperature $\left[\frac{T(r,t) - T_a}{T_m - T_a}\right]$

t = Time

r = Radial location

r_o = Motor radius

ξ = Normalized radial location (r/r_o)

ω = Circular frequency of container temperature variation

A = Normalized frequency $\sqrt{\frac{\omega r_o^2}{\alpha}}$

B = Biot number $\left[\frac{\bar{h} r_o}{k}\right]$

k = Motor thermal conductivity

ρ = Motor density

c = Motor specific heat

α = Motor thermal diffusivity $(k/\rho c)$

ber = Real Bessel function

bei = Imaginary Bessel function

$$X_r = \text{ber}_0(A) + \frac{A}{B\sqrt{2}}\,\text{ber}_1(A) + \frac{A}{B\sqrt{2}}\,\text{bei}_1(A)$$

$$X_i = \text{bei}_0(A) + \frac{A}{B\sqrt{2}}\,\text{bei}_1(A) - \frac{A}{B\sqrt{2}}\,\text{ber}_1(A)$$

$$\delta = \tan^{-1}\left[\frac{X_r \text{bei}_0(A\xi) - X_i \text{ber}_0(A\xi)}{X_r \text{ber}_0(A\xi) + X_i \text{bei}_0(A\xi)}\right]$$

θ_r = Temperature amplitude attenuation

$$\frac{\left[\text{ber}_0^2(A\xi) + \text{bei}_0^2(A\xi)\right]^{1/2}}{\left[X_r^2 + X_i^2\right]^{1/2}}$$

A parameter study was carried out on equation (10) with the assistance of an IBM 360 computer. Values of the temperature amplitude attenuation parameter, θ_r, and phase lag, δ, were determined at three normalized radial locations, ξ = 0.0, 0.5, and 1.0, for values of A and B of practical interest. Tables 5 through 9 present the results of this study. The phase lag, δ, is given in radians, where 2π radians equals one complete cycle. For environmental considerations, one complete cycle represents twenty-four hours.

For ease of use, the results of the parameter study are also presented in nomograph form in Figures 9 through 12. Temperature amplitude attenuation, θ_r, and phase lag, δ, are plotted parametrically against A and B at normalized radial locations of ξ = 0.0 and ξ = 1.0 (center and surface of motor, respectively).

TABLE 5

Values of Amplitude Attenuation Parameter, θ_r, and phase lag, δ, versus Biot Number, B, for a value of Normalized Frequency Parameter, A, equal to 1.0.

A	B	DISTANCE FROM CENTER	TIME DELAY IN RADIANS	RELATIVE AMPLITUDE
1.0	0.1	0.0	-1.50	0.19
1.0	0.1	0.5	-1.44	0.19
1.0	0.1	1.0	-1.25	0.19
1.0	0.5	0.0	-0.97	0.66
1.0	0.5	0.5	-0.90	0.66
1.0	0.5	1.0	-0.72	0.67
1.0	1.0	0.0	-0.68	0.84
1.0	1.0	0.5	-0.62	0.84
1.0	1.0	1.0	-0.43	0.86
1.0	2.0	0.0	-0.48	0.93
1.0	2.0	0.5	-0.42	0.93
1.0	2.0	1.0	-0.23	0.94
1.0	3.0	0.0	-0.41	0.95
1.0	3.0	0.5	-0.34	0.95
1.0	3.0	1.0	-0.16	0.97
1.0	4.0	0.0	-0.37	0.96
1.0	4.0	0.5	-0.31	0.96
1.0	4.0	1.0	-0.12	0.98
1.0	5.0	0.0	-0.34	0.97
1.0	5.0	0.5	-0.28	0.97
1.0	5.0	1.0	-0.10	0.98
1.0	10.0	0.0	-0.30	0.98
1.0	10.0	0.5	-0.23	0.98
1.0	10.0	1.0	-0.05	0.99
1.0	50.0	0.0	-0.26	0.98
1.0	50.0	0.5	-0.20	0.98
1.0	50.0	1.0	-0.01	1.00
1.0	100.0	0.0	-0.25	0.98
1.0	100.0	0.5	-0.19	0.99
1.0	100.0	1.0	-0.00	1.00

TABLE 6

Values of Amplitude Attenuation Parameter, θ_r, and phase lag, δ, versus Biot Number, B, for a value of Normalized Frequency Parameter, A, equal to 2.0.

A	B	DISTANCE FROM CENTER	TIME DELAY IN RADIANS	RELATIVE AMPLITUDE
2.0	0.1	0.0	-2.01	0.05
2.0	0.1	0.5	-1.76	0.05
2.0	0.1	1.0	-1.10	0.06
2.0	0.5	0.0	-1.83	0.21
2.0	0.5	0.5	-1.58	0.21
2.0	0.5	1.0	-0.92	0.26
2.0	1.0	0.0	-1.65	0.36
2.0	1.0	0.5	-1.41	0.36
2.0	1.0	1.0	-0.74	0.44
2.0	2.0	0.0	-1.43	0.52
2.0	2.0	0.5	-1.19	0.53
2.0	2.0	1.0	-0.52	0.64
2.0	3.0	0.0	-1.31	0.61
2.0	3.0	0.5	-1.06	0.62
2.0	3.0	1.0	-0.40	0.75
2.0	4.0	0.0	-1.23	0.66
2.0	4.0	0.5	-0.98	0.67
2.0	4.0	1.0	-0.32	0.81
2.0	5.0	0.0	-1.18	0.69
2.0	5.0	0.5	-0.93	0.70
2.0	5.0	1.0	-0.27	0.85
2.0	10.0	0.0	-1.06	0.75
2.0	10.0	0.5	-0.81	0.77
2.0	10.0	1.0	-0.14	0.93
2.0	50.0	0.0	-0.94	0.80
2.0	50.0	0.5	-0.69	0.81
2.0	50.0	1.0	-0.03	0.99
2.0	100.0	0.0	-0.93	0.81
2.0	100.0	0.5	-0.68	0.82
2.0	100.0	1.0	-0.02	0.99

TABLE 7

Values of Amplitude Attenuation Parameter, θ_r, and phase lag, δ, versus Biot Number, B, for a value of Normalized Frequency Parameter, A, equal to 3.0.

A	B	DISTANCE FROM CENTER	TIME DELAY IN RADIANS	RELATIVE AMPLITUDE
3.0	0.1	0.0	-2.60	0.02
3.0	0.1	0.5	-2.06	0.02
3.0	0.1	1.0	-0.92	0.04
3.0	0.5	0.0	-2.50	0.08
3.0	0.5	0.5	-1.95	0.09
3.0	0.5	1.0	-0.81	0.16
3.0	1.0	0.0	-2.39	0.15
3.0	1.0	0.5	-1.85	0.16
3.0	1.0	1.0	-0.71	0.29
3.0	2.0	0.0	-2.24	0.24
3.0	2.0	0.5	-1.70	0.26
3.0	2.0	1.0	-0.56	0.47
3.0	3.0	0.0	-2.14	0.30
3.0	3.0	0.5	-1.59	0.32
3.0	3.0	1.0	-0.45	0.58
3.0	4.0	0.0	-2.06	0.34
3.0	4.0	0.5	-1.52	0.36
3.0	4.0	1.0	-0.38	0.66
3.0	5.0	0.0	-2.01	0.37
3.0	5.0	0.5	-1.47	0.39
3.0	5.0	1.0	-0.33	0.72
3.0	10.0	0.0	-1.88	0.43
3.0	10.0	0.5	-1.33	0.47
3.0	10.0	1.0	-0.19	0.84
3.0	50.0	0.0	-1.73	0.50
3.0	50.0	0.5	-1.18	0.53
3.0	50.0	1.0	-0.04	0.97
3.0	100.0	0.0	-1.71	0.50
3.0	100.0	0.5	-1.16	0.54
3.0	100.0	1.0	-0.02	0.98

TABLE 8

Values of Amplitude Attenuation Parameter, θ_r, and phase lag, δ, versus Biot Number, B, for a value of Normalized Frequency Parameter, A, equal to 4.0.

A	B	DISTANCE FROM CENTER	TIME DELAY IN RADIANS	RELATIVE AMPLITUDE
4.0	0.1	0.0	-3.28	0.01
4.0	0.1	0.5	-2.36	0.01
4.0	0.1	1.0	-0.86	0.03
4.0	0.5	0.0	-3.20	0.04
4.0	0.5	0.5	-2.29	0.04
4.0	0.5	1.0	-0.79	0.12
4.0	1.0	0.0	-3.12	0.07
4.0	1.0	0.5	-2.21	0.08
4.0	1.0	1.0	-0.71	0.23
4.0	2.0	0.0	-2.99	0.11
4.0	2.0	0.5	-2.08	0.14
4.0	2.0	1.0	-0.58	0.39
4.0	3.0	0.0	-2.90	0.14
4.0	3.0	0.5	-1.99	0.18
4.0	3.0	1.0	-0.49	0.50
4.0	4.0	0.0	-2.84	0.17
4.0	4.0	0.5	-1.92	0.21
4.0	4.0	1.0	-0.42	0.58
4.0	5.0	0.0	-2.78	0.18
4.0	5.0	0.5	-1.87	0.23
4.0	5.0	1.0	-0.37	0.64
4.0	10.0	0.0	-2.64	0.23
4.0	10.0	0.5	-1.73	0.28
4.0	10.0	1.0	-0.23	0.79
4.0	50.0	0.0	-2.47	0.28
4.0	50.0	0.5	-1.55	0.34
4.0	50.0	1.0	-0.05	0.95
4.0	100.0	0.0	-2.44	0.28
4.0	100.0	0.5	-1.53	0.35
4.0	100.0	1.0	-0.03	0.98

TABLE 9

Values of Amplitude Attenuation Parameter, θ_r, and phase lag, δ, versus Biot Number, B, for a value of Normalized Frequency Parameter, A, equal to 5.0.

A	B	DISTANCE FROM CENTER	TIME DELAY IN RADIANS	RELATIVE AMPLITUDE
5.0	0.1	0.0	-3.97	0.00
5.0	0.1	0.5	-2.67	0.01
5.0	0.1	1.0	-0.85	0.02
5.0	0.5	0.0	-3.91	0.02
5.0	0.5	0.5	-2.61	0.02
5.0	0.5	1.0	-0.79	0.10
5.0	1.0	0.0	-3.85	0.03
5.0	1.0	0.5	-2.54	0.05
5.0	1.0	1.0	-0.72	0.19
5.0	2.0	0.0	-3.74	0.05
5.0	2.0	0.5	-2.44	0.08
5.0	2.0	1.0	-0.62	0.32
5.0	3.0	0.0	-3.66	0.07
5.0	3.0	0.5	-2.35	0.10
5.0	3.0	1.0	-0.53	0.43
5.0	4.0	0.0	-3.59	0.08
5.0	4.0	0.5	-2.29	0.12
5.0	4.0	1.0	-0.47	0.51
5.0	5.0	0.0	-3.54	0.09
5.0	5.0	0.5	-2.24	0.14
5.0	5.0	1.0	-0.42	0.57
5.0	10.0	0.0	-3.39	0.12
5.0	10.0	0.5	-2.09	0.18
5.0	10.0	1.0	-0.27	0.74
5.0	50.0	0.0	-3.19	0.15
5.0	50.0	0.5	-1.89	0.23
5.0	50.0	1.0	-0.07	0.94
5.0	100.0	0.0	-3.16	0.16
5.0	100.0	0.5	-1.85	0.24
5.0	100.0	1.0	-0.03	0.97

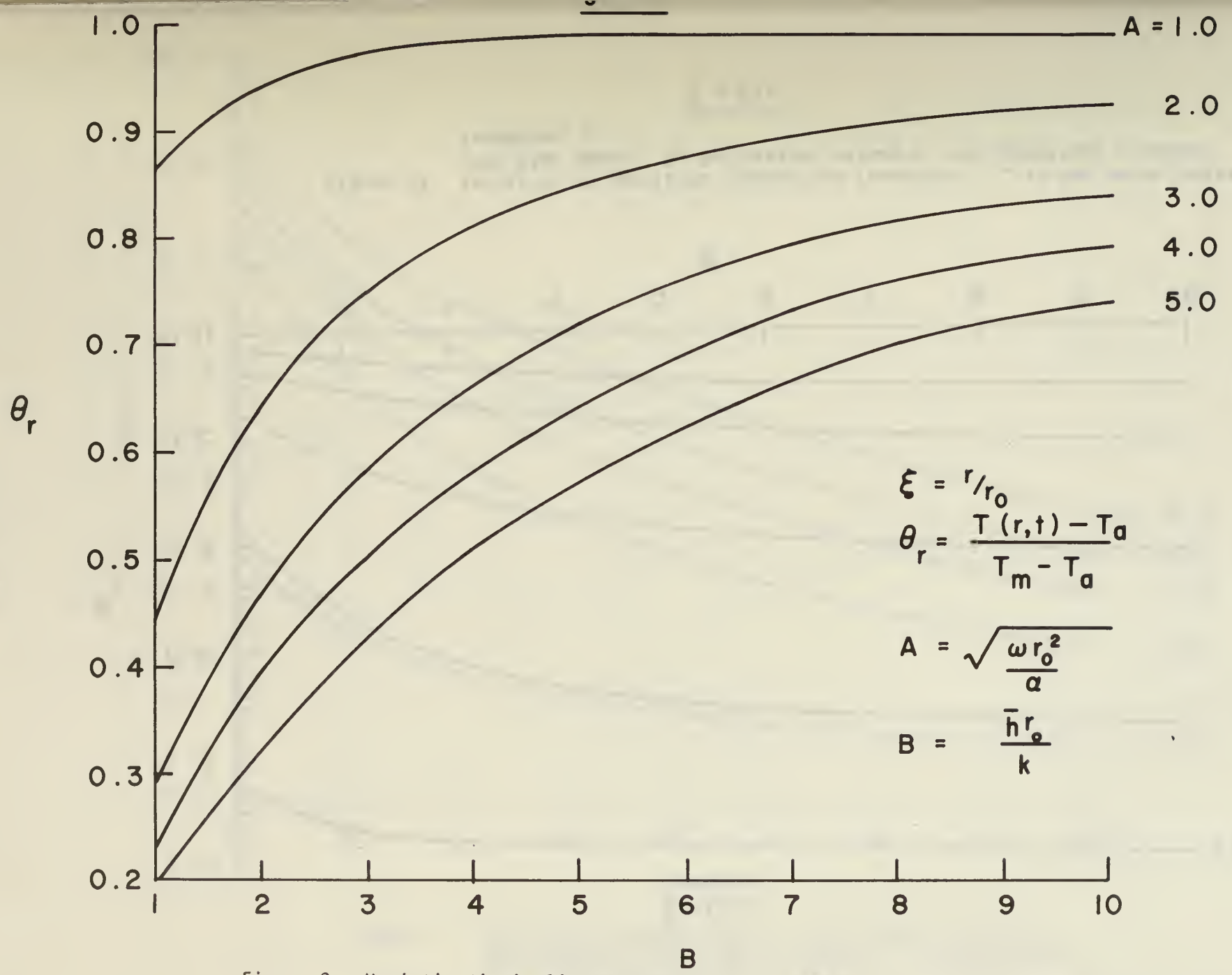

Figure 9. Variation in Amplitude Attenuation Parameter, θ_r, on the Motor Skin, with Biot Number, B, for various values of the Normalized Frequency Parameter, A.

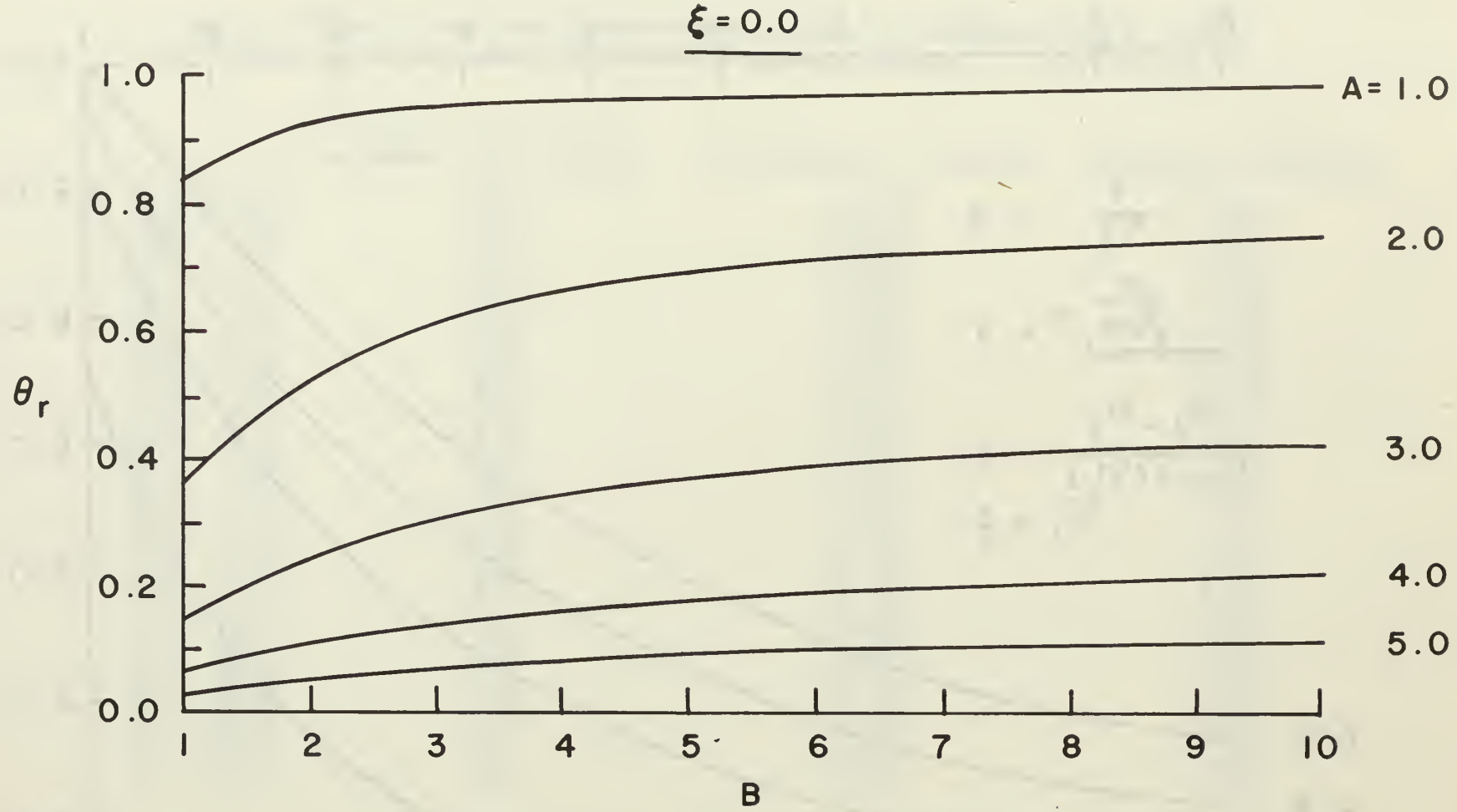

Figure 10. Variation in Amplitude Attenuation Parameter, θ_r, at the Motor Center, with Biot number, B, for various values of the Normalized Frequency Parameter, A.

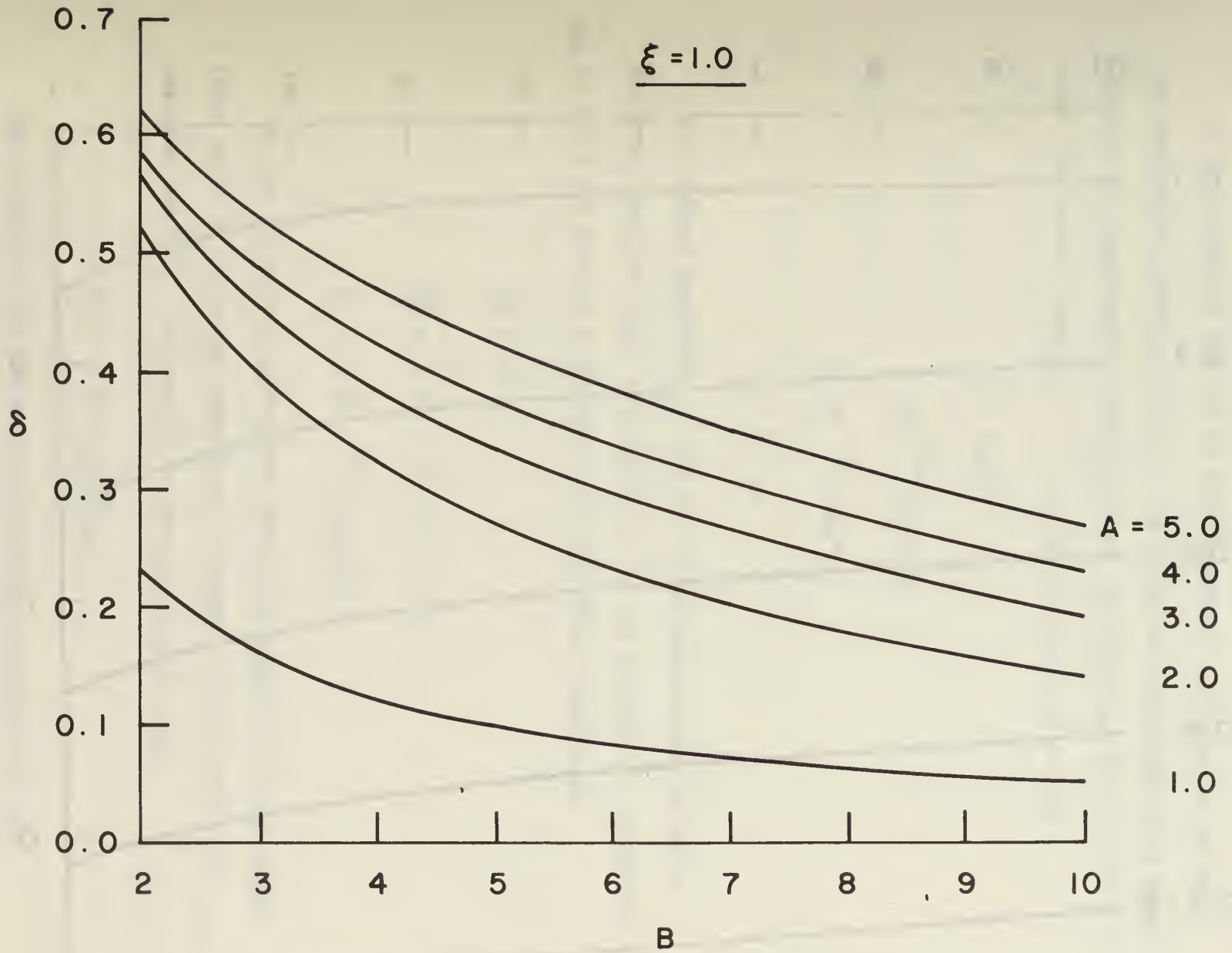

Figure 11. Variation in Phase Lag, δ, on the Motor Skin, with Biot number, B, for various values of the Normalized Frequency Parameter, A.

Figure 12. Variation in Phase Lag, δ at the Motor Center, with Biot number, B, for various values of the Normalized Frequency Parameter, A.

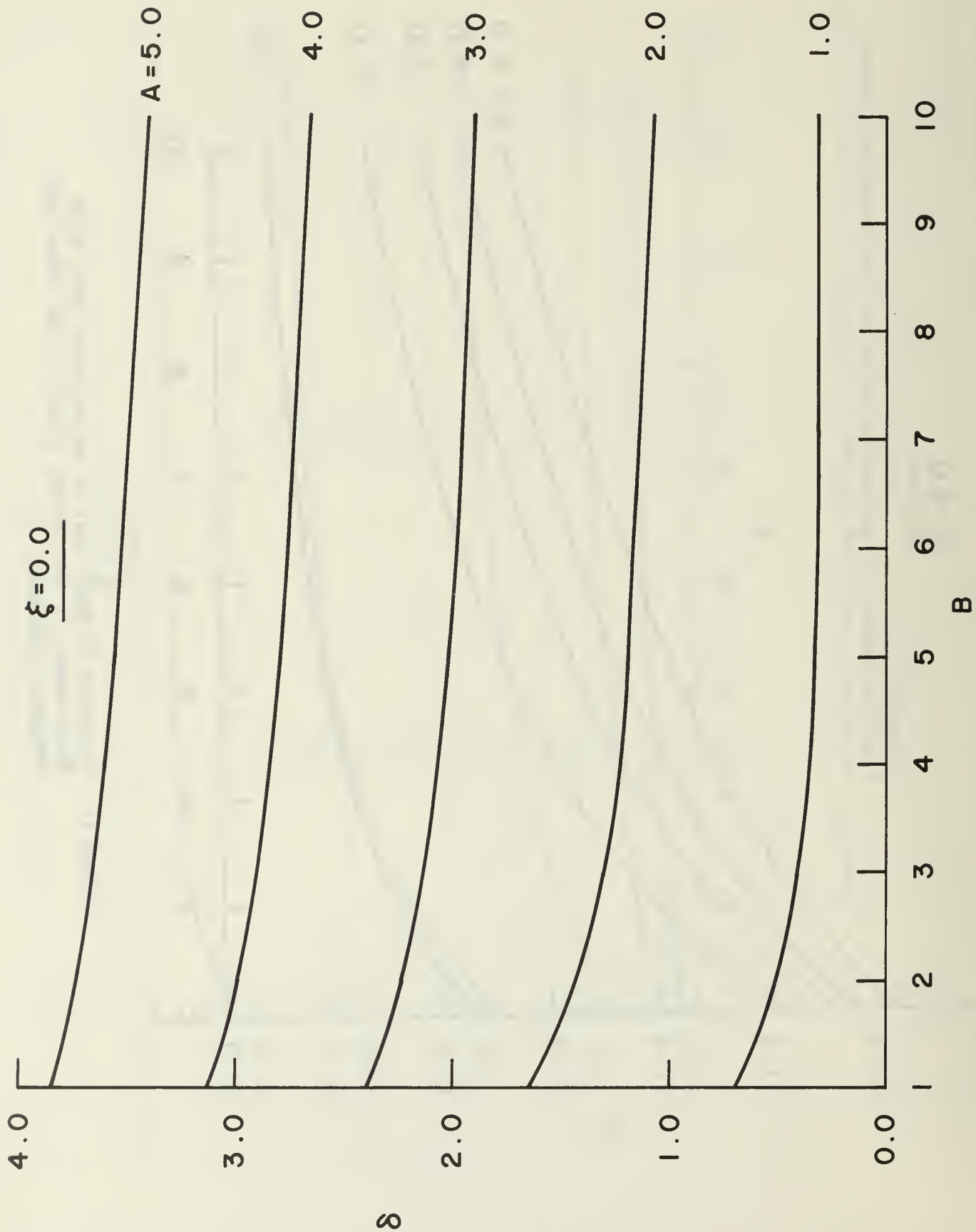

C. Sample Calculation

As an example of the use of the temperature attenuation and phase lag nomographs, consideration will be given the once-fired ASROC motor used in the experimental investigation. The motor was filled with dry, wind blown sand. Reference 4 lists the properties of sand as:

$$\rho = 94.8 \text{ lbm/ft}^3$$

$$k = 0.188 \text{ BTU/hr-ft-°F}$$

$$c = 0.195 \text{ BTU/lbm-°F}$$

$$\alpha = 0.01 \text{ ft}^2\text{/hr}$$

The thermal properties of the air in the gap between the motor and container were taken from reference 5. An average air temperature of 100°F was used as a representative reference temperature.

$$Pr = 0.72$$

$$\frac{g\beta}{\nu^2} = 1.76 \times 10^6 \text{ (°F - ft}^3\text{)}^{-1}$$

$$k_g = 0.0154 \text{ BTU/hr-ft-°F}$$

The gap convective coefficient defined by equation (9) was calculated using an estimated temperature difference between motor and container of 10°F. The results of the calculation yield:

$$h_c = 0.20 \frac{\text{BTU}}{\text{hr-ft}^2\text{-°F}}$$

The linearized gap radiation coefficient, equation (8), was calculated using the following values:

$r_1 = 0.5$ ft.

$r_2 = 0.75$ ft.

$\sigma = 0.1714 \times 10^{-8} \quad \frac{BTU}{hr\text{-}ft^2\text{-}°R^4}$

$T_1 \simeq 100°F = 560°R$ (average motor temperature)

$T_2 \simeq 100°F = 560°R$ (average container temperature)

$\varepsilon_1 = \varepsilon_2 = 0.9$ (typical emissivities for grey painted surfaces)

$$F_{1\text{-}2} = \frac{1}{\frac{1}{\varepsilon_1} + \frac{r_1}{r_2}\left(\frac{1}{\varepsilon_2} - 1\right)} = 0.84 \text{ (ref. 5, p. 260)}$$

Substituting these values into equation (8), one finds

$$h_r = 1.05 \quad \frac{BTU}{hr\text{-}ft^2\text{-}°F}$$

Using the calculated values of h_r and h_c, the overall gap conductance is found to be:

$$\bar{h} = h_r + h_c$$

$$\simeq 1.25 \quad \frac{BTU}{hr\text{-}ft^2\text{-}°F}$$

The frequency parameter, A, and Biot number, B, are now easily calculated as A = 2.60 and B = 3.35. In calculating A, the circular frequency was assumed to equal $2\pi/24 = 0.262 \ \frac{radians}{hour}$.

Now, referring to Figures 9 through 12, the following values are found:

$$\xi = 0.0,\ \theta_r = 0.42 \quad \delta = -1.8 \text{ radians} \tag{12}$$

$$\xi = 1.0,\ \theta_r = 0.67 \quad \delta = -0.39 \text{ radians} \tag{13}$$

Substituting the above values into equation (11) we find:

At $\xi = 0$ (motor center)

$$\frac{(T(o,t) - T_a)}{(T_m - T_a)} = 0.42 \sin(\omega t - 1.8) \tag{14}$$

At $\xi = 1.0$ (motor skin)

$$\frac{(T(r_o,t) - T_a)}{(T_m - T_a)} = 0.67 \sin(\omega t - 0.39) \tag{15}$$

To convert θ_r and δ to dimensional temperature and time, we must specify the following information:

1. The duration of one complete cycle.
2. The maximum container bulk temperature.
3. The minimum container bulk temperature.
4. The average container bulk temperature.

As an example, using the experimental results obtained on August 2, 1972 (Table 2), we find that one complete cycle is equivalent to twenty-four hours and the maximum and minimum container bulk temperatures are 138°F and 64°F, respectively. These temperatures, when averaged, yield an average container temperature of 101°F. Substituting these results into equations (14) and (15) and rearranging in dimensional form, one finds:

At r = 0.0 ft. (center of motor),

$$T(o,t) = 15.5 \sin\{(0.26)\ (t - 6.9)\} + 101 \quad (°F) \tag{16}$$

At r = 0.5 ft (surface of motor),

$$T(r_o,t) = 25 \sin \{(0.26)\ (t-1.5)\} + 101 \quad (°F) \qquad (17)$$

Figure 13 shows plots of equations (16) and (17) together with the assumed container bulk temperature variation. The important points to note are:

1. Maximum and minimum container bulk temperatures of 138°F and 64°F, respectively, lead to predicted maximum and minimum temperatures at the motor center of 116.5°F and 84.5°F, respectively, and at the motor surface of 126°F and 76°F, respectively.
2. The thermal time lag at the rocket motor center is predicted to be 6.9 hours while that at the motor surface is 1.5 hours.

VI. COMPARISON OF THEORY WITH EXPERIMENT

Figures 14 and 15 show comparisons of theoretically predicted temperatures with experimental results obtained on August 2, 1972. The experimentally determined container bulk temperature variation was used as the forcing function in the theory. Figure 14 represents the bulk temperature variation at the surface of the motor while Figure 15 represents the temperature variation at the center of the motor.

Table 10 compares theoretical amplitude and phase shift predictions at the motor center and skin with experimental results. As can be seen, the comparison is excellent with the exception of the phase shift comparisons at the motor center. An uncertainty analysis has been performed on both the experiment and theory (the uncertainty in the theory is a

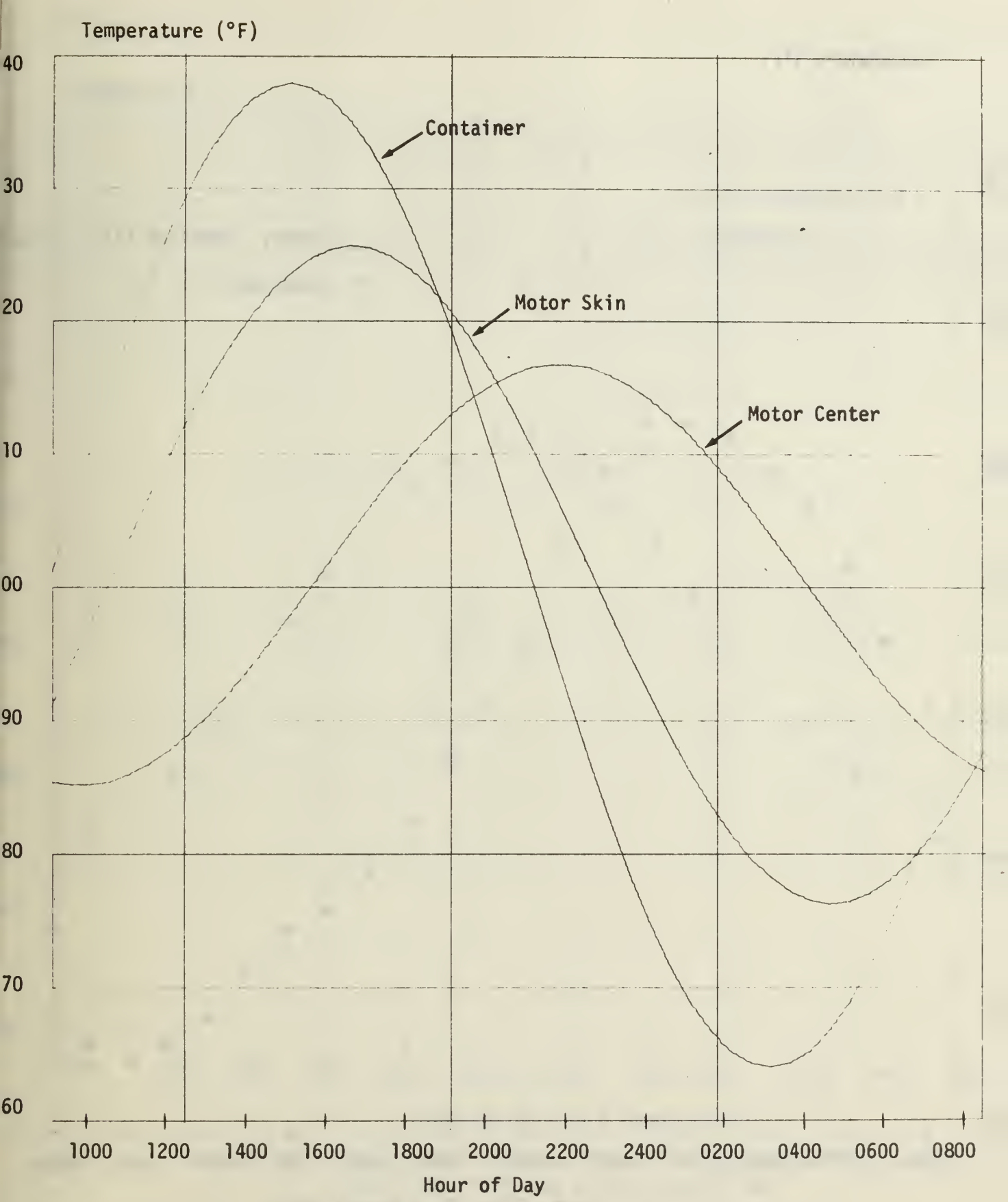

Figure 13. Analytical Predictions of Temperature Variation with Time at surface and center of ASROC motor.

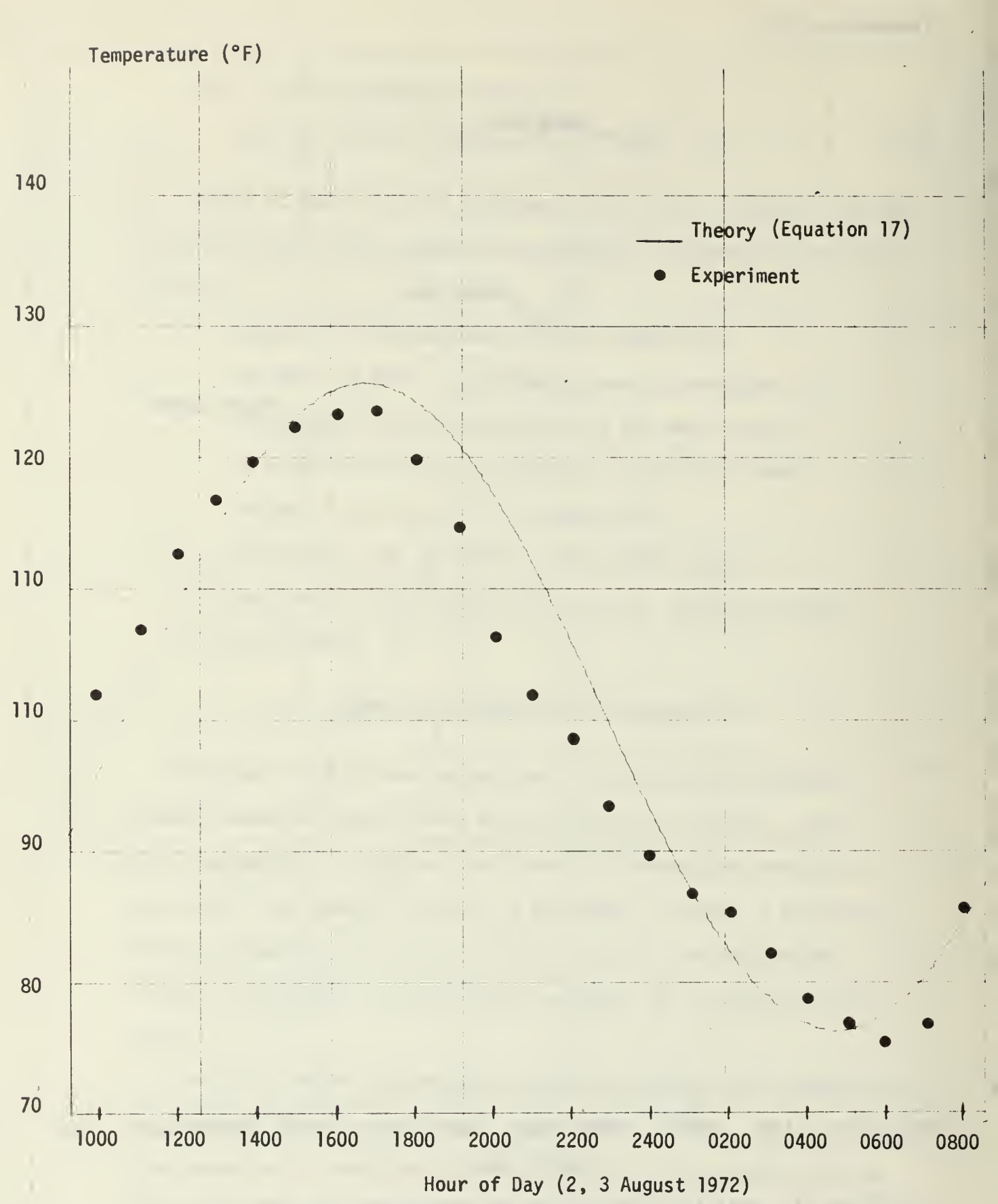

Figure 14. Comparison of Measured Values of Motor Skin Temperatures with Values Predicted Using Equation 17.

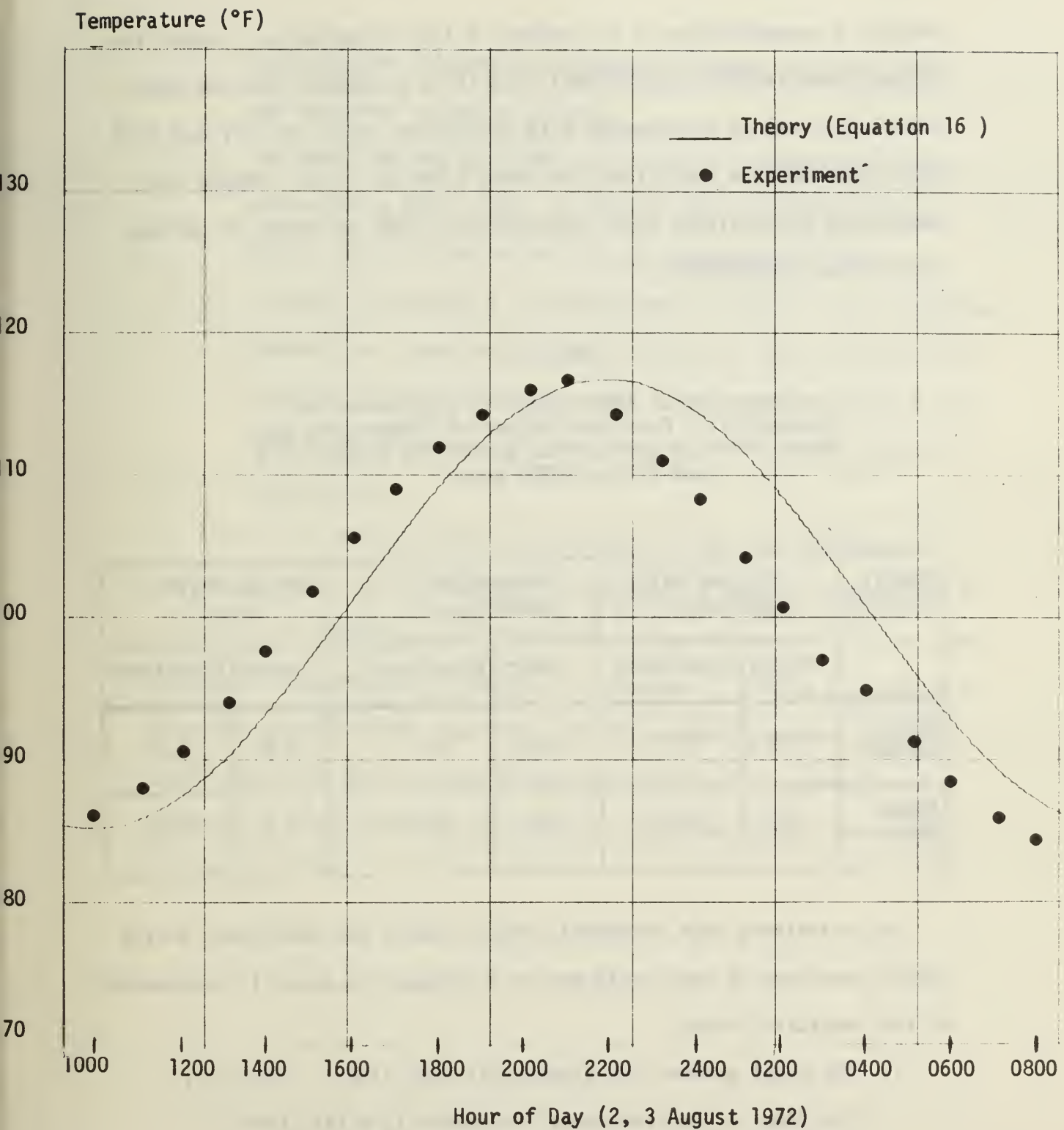

Figure 15. Comparison of Measured Values of Motor Center Temperatures with Values Predicted Using Equation 16.

result of uncertainties in the values of the thermophysical properties of sand used in the calculations), and it is estimated that the total uncertainty may be represented with uncertainty bands of ±3°F and ±0.5 hours on each data point (see reference 2 for details). Theory and experiment agree within these uncertainty limits at values of maximum and minimum temperature.

Table 10

Comparison of Experimentally Determined and Theoretically Predicted Values of Temperature and Phase Shift on the Surface and in the Center of a Sand-filled ASROC motor

Radial Location	Maximum Bulk Temperature (°F)		Minimum Bulk Temperature °F		Phase Shift (hours)	
	Theory	Experiment	Theory	Experiment	Theory	Experiment
Motor Center	116.5	117	84.5	84	6.9	5.3
Motor Skin	126	123	76	75	1.5	1.6

The relatively poor agreement between theory and experiment during certain portions of each cycle may be attributed to several shortcomings of the analytical model:

1. The model assumes one dimensional heat flow. In reality, the flow is two dimensional and possibly mildly three dimensional.
2. The model assumes that the gap conductance is constant. In reality, the gap conductance varies with time due to the

fact that the temperature difference between the motor skin and container varies with time.

3. The model assumes that the bulk container temperature varies sinusoidally with time. In reality, the variation is not truly sinusoidal as can be seen by examining Figure 8.
4. In order to develop a one-dimensional solution, a bulk container temperature, Equation (3), was defined and used as the forcing function in the theoretical model. This bulk temperature only partially compensates for the truly two dimensional nature of the problem.

All of the aforementioned shortcomings of the one-dimensional analytical model can be overcome by employing a numerical procedure to solve for the temperature distribution in the ordnance. This has been done and is reported on in detail in reference 2. While the numerical solution yields results that very closely approximate those obtained experimentally, the increase in time and effort is considerable when compared to the simplicity of using the analytical model, especially in nomograph form.

VII. CONCLUSIONS AND RECOMMENDATIONS

Based on the results of our investigation we offer the following conclusions and recommendations:

1. Although a sine wave is not a perfect fit to the actual container temperature variation at all points in time, it is useful for predicting bulk temperatures and thermal time lags throughout the rocket motor, especially if only high and low bulk temperatures are of interest.

2. The simplicity of the analytical model, as presented in nomograph form, allows parameter studies to be quickly and easily carried out. The results of our study should prove to be a useful tool to aide in the future design of thermally optimized containers.

3. Our theoretical model has been verified by comparison with experimental results obtained on a container stored ASROC motor. Additional comparisons should be made with data obtained on other types of container stored ordnance. Vast amounts of experimental data have been obtained on a variety of ordnance and are available for comparison [6]. However, before our model can be employed, a method for obtaining meaningful container bulk temperature variations must be developed. Virtually all existing data, with the exception of that presented herein, were taken at the 12 o'clock locations on the container and motor. While these temperatures represent extremes, or near extremes, they are not truly representative of bulk temperatures. A technique is needed for estimating maximum and minimum bulk temperatures based on a knowledge of only the temperatures taken at the 12 o'clock locations

and the measured ambient temperature, the measured ambient temperature being somewhat representative of the temperature at the 6 o'clock location on the container. As an example, Table 4 compares the actual bulk temperature of the ASROC container used in the present studies with an estimated bulk temperature calculated by simply averaging the temperature measured at the 12 o'clock location with the ambient air temperature. We do not necessarily recommend this scheme in preference to other schemes but simply offer it as an example. Perhaps a weighted averaging technique would yield closer agreement as the straight averaging technique does not yield close comparisons at all points in time, especially near peak temperatures.

4. Table 4 presents a comparison of the temperatures measured at the 12 o'clock locations on the container which contained an ASROC motor with a container that was empty. Close inspection of the data indicate that there is very little difference in the temperatures measured on the two. This suggests that an empty storage container may be used to obtain container temperature data for use in the analytical model.

5. The analytical model presented herein uses, as a forcing function, experimentally determined values of the container temperature. It is recommended that a study be conducted to develop predictions of the container surface temperature as a function of solar irradiation, terrestial irradiation, wind velocity, and ambient air temperature.

REFERENCES

1. Arpaci, V. S., Conduction Heat Transfer, pp. 324-328, Addison-Wesley, 1966.

2. Wirzburger, A. H., An Environmental Heat Transfer Study of a Rocket Motor Storage Container System, M. S. Thesis, Naval Postgraduate School, Monterey, California, December 1972.

3. Liu, C. Y., Mueller, W. K. and Landis, F., Natural Convection Heat Transfer in Long Horizontal Cylindrical Annuli, International Developments in Heat Transfer, Part V, pp. 976-984, 1961.

4. Baumeister, T., Marks Standard Handbook for Mechanical Engineers, 7th Edition, pp. 4-11, 4-95, 4-111, McGraw Hill, 1967.

5. Kreith, F., Principles of Heat Transfer, 3rd Ed., p. 636, Intext Educational Publishers, 1973.

6. Schafer, H. C., Measured Temperatures of Solid Rocket Motors Dump Stored in the Tropics and Desert, Naval Weapons Center Tech. Pub. 5039, Nov. 1972, Parts 1 and 2.

INITIAL DISTRIBUTION LIST

	No. Copies
1. Commander Naval Weapons Center China Lake, California 93555 Attn:	
Mr. R. G. Christiansen (Code 45332)	1
Mr. T. Inouye (Code 4533)	30
Mr. C. Maples (Code 453)	1
Mr. C. F. Markarian (Code 4061)	1
Mr. H. C. Schafer (Code 45330)	5
Dr. R. Ulrich (Code 4570)	1
2. Library Naval Postgraduate School Monterey, California 93940	2
3. Dean of Research Naval Postgraduate School Monterey, California 93940	2
4. Director Defense Documentation Center 5010 Duke Street Alexandria, Virginia 22314	20
5. Department of Mechanical Engineering, Code 59 Naval Postgraduate School Monterey, California 93940	1
6. Professor Thomas E. Cooper, Code 59Cg Naval Postgraduate School Monterey, California 93940	10
7. LCDR Allen H. Wirzburger, Code 59 Naval Postgraduate School Monterey, California 93940	5

DOCUMENT CONTROL DATA - R & D

(Security classification of title, body of abstract and indexing annotation must be entered when the overall report is classified)

1. ORIGINATING ACTIVITY (Corporate author)
Naval Postgraduate School
Monterey, California 93940

2a. REPORT SECURITY CLASSIFICATION
Unclassified

2b. GROUP

3. REPORT TITLE
An Analytical Model for Predicting the Daily Temperature Cycle of Container Stored Ordnance

4. DESCRIPTIVE NOTES (Type of report and inclusive dates)
Final Report, 1972-73

5. AUTHOR(S) (First name, middle initial, last name)
Thomas E. Cooper
Allen H. Wirzburger

6. REPORT DATE
18 June 1973

7a. TOTAL NO. OF PAGES
61

7b. NO. OF REFS
6

8a. CONTRACT OR GRANT NO

b. PROJECT NO.

c. Work Request No. 3-3006
Naval Weapons Center, China Lake,
d. California.

9a. ORIGINATOR'S REPORT NUMBER(S)
NPS - 59CG73061A

9b. OTHER REPORT NO(S) (Any other numbers that may be assigned this report)

10. DISTRIBUTION STATEMENT
This document has been approved for public release and sale; its distribution is unlimited.

11. SUPPLEMENTARY NOTES

12. SPONSORING MILITARY ACTIVITY
Naval Weapons Center
China Lake
California 93555

13. ABSTRACT

The heat transfer characteristics of a container stored rocket motor have been investigated using analytical and experimental techniques. Comparison between analytically predicted and experimentally determined values of temperature are within the estimated experimental uncertainty of ±3°F. The results of the analytical solution may be used to predict maximum and minimum temperatures, thermal time lags, and temperature gradients throughout the rocket motor. For convenience, maximum temperature and time lag information is presented in nomograph form as a function of three parameters: normalized radial location, normalized frequency, and normalized gap conductance. These three parameters control the temperature behavior of the motor. It is proposed that the nomographs will be a useful tool for thermally optimizing future container designs.

14 KEY WORDS	LINK A		LINK B		LINK C	
	ROLE	WT	ROLE	WT	ROLE	WT
Heat Transfer						
Conduction						
Radiation						
Convection						
Ordnance						
Concentric Cylinders						
Dump Storage						
Environmental Effects						
Liquid Crystals						